Journal of Rock Mechanics and Geotechnical Engineering 15 (2023) 2954–2972

Contents lists available at ScienceDirect

Journal of Rock Mechanics and Geotechnical Engineering

journal homepage: www.jrmge.cn

Full Length Article

Uncertainties of landslide susceptibility prediction considering different landslide types

Faming Huang [a,b], Haowen Xiong [a,b], Chi Yao [a,*], Filippo Catani [c], Chuangbing Zhou [a], Jinsong Huang [d]

[a] School of Infrastructure Engineering, Nanchang University, Nanchang, 330031, China
[b] Jiangxi Provincial Key Laboratory of Interdisciplinary Science, Nanchang University, Nanchang, 330031, China
[c] Department of Geosciences, University of Padova, Padova, Italy
[d] Discipline of Civil, Surveying and Environmental Engineering, Priority Research Centre for Geotechnical Science and Engineering, University of Newcastle, NSW, 2287, Australia

ARTICLE INFO

Article history:
Received 17 October 2022
Received in revised form
22 February 2023
Accepted 12 March 2023
Available online 20 March 2023

Keywords:
Landslide susceptibility
Landslide type
Rock fall
Colluvial landslides
Machine learning models

ABSTRACT

Most literature related to landslide susceptibility prediction only considers a single type of landslide, such as colluvial landslide, rock fall or debris flow, rather than different landslide types, which greatly affects susceptibility prediction performance. To construct efficient susceptibility prediction considering different landslide types, Huichang County in China is taken as example. Firstly, 105 rock falls, 350 colluvial landslides and 11 related environmental factors are identified. Then four machine learning models, namely logistic regression, multi-layer perception, support vector machine and C5.0 decision tree are applied for susceptibility modeling of rock fall and colluvial landslide. Thirdly, three different landslide susceptibility prediction (LSP) models considering landslide types based on C5.0 decision tree with excellent performance are constructed to generate final landslide susceptibility: (i) united method, which combines all landslide types directly; (ii) probability statistical method, which couples analyses of susceptibility indices under different landslide types based on probability formula; and (iii) maximum comparison method, which selects the maximum susceptibility index through comparing the predicted susceptibility indices under different types of landslides. Finally, uncertainties of landslide susceptibility are assessed by prediction accuracy, mean value and standard deviation. It is concluded that LSP results of the three coupled models considering landslide types basically conform to the spatial occurrence patterns of landslides in Huichang County. The united method has the best susceptibility prediction performance, followed by the probability method and maximum susceptibility method. More cases are needed to verify this result in-depth. LSP considering different landslide types is superior to that taking only a single type of landslide into account.

© 2023 Institute of Rock and Soil Mechanics, Chinese Academy of Sciences. Production and hosting by Elsevier B.V. This is an open access article under the CC BY-NC-ND license (http://creativecommons.org/licenses/by-nc-nd/4.0/).

1. Introduction

Landslides are one of the most common types of geological disasters worldwide, causing a lot of casualties and economic losses every year (Di Napoli et al., 2021; He et al., 2021). Modeling of landslide susceptibility prediction (LSP) based on remote sensing and geographic information system (GIS) platform can predict the spatial distribution of landslides and is beneficial to the landslide prevention. Therefore, reliable LSP modeling is of great significance.

The landslide inventory information is one of the most important data basis for LSP modeling, as well as the model output variables and the object of model training and testing. Generally speaking, a landslide is a physical system with several stages of evolution. According to the Varnes landslide classification system, landslides can be classified as colluvial landslides, rock fall, debris flow, rolling rocks, rock landslides, etc. (Hungr et al., 2014), which present different physical, mechanical and evolutional characteristics. Obviously, there are some differences in the corresponding LSP process (Farzam et al., 2018).

* Corresponding author.
E-mail address: chi.yao@ncu.edu.cn (C. Yao).

Peer review under responsibility of Institute of Rock and Soil Mechanics, Chinese Academy of Sciences.

https://doi.org/10.1016/j.jrmge.2023.03.001

1674-7755 © 2023 Institute of Rock and Soil Mechanics, Chinese Academy of Sciences. Production and hosting by Elsevier B.V. This is an open access article under the CC BY-NC-ND license (http://creativecommons.org/licenses/by-nc-nd/4.0/).

Literature review shows that most of the existing LSP modeling is based on a single type of landslide without considering the impact of different landslide types, or in the modeling process, it is not specified whether the characteristics of different landslide types are distinguished. That is to say, there are few LSP studies built from the perspective of coupling various types of landslides (Guzzetti et al., 1999; Brenning, 2005; Huang and Zhao, 2018; Reichenbach et al., 2018; Merghadi et al., 2020). As is known to all, different types of landslides also have some differences in evolution characteristics and instability mechanisms (Hungr et al., 2014). In field condition, different landslide types or multiple types of landslides may occur at a specific location (Guo et al., 2019). For example, Sun et al. (2020a) classified landslides into soil landslides and rock landslides according to the landslide characteristics in Xining City of China. This research showed that LSP under different landslide types were not consistent in terms of modeling characteristics. As a result, it is of great significance to construct a LSP model that can consider different landslide types (Zhou et al., 2018).

In this paper, a LSP model considering landslide types is constructed to explore the characteristics and patterns of LSP models. Based on the literature review and basic principles of probability statistics, three coupled methods for LSP models that consider different landslide types are proposed:

(1) United method, which does not distinguish landslide types, and the common frequency ratios of all landslide types in the study area are calculated in the input variable processing stage to directly predict landslide susceptibility (Jiang et al., 2017; Wang et al., 2021).
(2) Probability statistics method, which is based on the correlation coefficient between different types of landslides. The probability formula is used for coupling analysis of the predicted susceptibility indices under different types of landslides and calculating the final landslide susceptibility indices.
(3) Maximum comparison method, which compares the predicted susceptibility indices under different types of landslides, and selects the maximum susceptibility index as the final landslide susceptibility index (Zhou et al., 2018; Guo et al., 2019).

Considering the influence of different landslide types on LSP modeling, existing research shows that different data-driven models may produce many uncertainties in LSP modeling (Akgun, 2012; Aditian et al., 2018; Bui et al., 2020). In order to avoid the uncertainty caused by different machine learning models and improve the LSP accuracy, four types of machine learning models, including logistic regression (LR) (Chen et al., 2018), multi-layer perceptron (MLP) (Liu et al., 2021), support vector machine (SVM) (Kalantar et al., 2017; Zhang et al., 2022) and C5.0 decision tree (Golkarian et al., 2018), are used to predict LSP considering different landslide types.

Taking Huichang County in China as an example, the landslides in this area are mainly rock fall and colluvial landslides. Therefore, this paper mainly considers these two landslide types using the above three coupled methods for LSP. A type of efficient machine learning model is combined with these three coupled methods to carry out LSP considering different landslide types.

2. Methodologies

2.1. Modeling process of LSP

In this study, the formation mechanisms of rock fall and colluvial landslides are analyzed. Then the machine learning model with the best performance is combined with the unified method, the probability method, and the maximum susceptibility method, respectively, to build a LSP model considering landslide types. Finally, the uncertainty of LSP results is explored (Fig. 1):

(1) Data set preparation. Data sources of different types of landslides in Huichang County are obtained, including landslide inventory information, digital elevation model (DEM) data, remote sensing data and field surveys. A total of 11 environmental factors of rock fall and colluvial landslides in the study area are extracted by ArcGIS 10.3 and remote sensing software.
(2) The frequency ratios of rock fall and colluvial landslides are calculated as the input variables of the four machine learning models, namely LR, MLP, SVM and C5.0 decision tree models. The susceptibility prediction of rock fall and colluvial landslide is further carried out.
(3) From the perspectives of frequency ratio accuracy, susceptibility index distribution pattern and area under receiver operation characteristic curve (AUC) accuracy, the susceptibility prediction performance of rock fall and colluvial landslides under four machine learning models are evaluated. Then the model with the best performance is combined with the unified method, the probability method, and the maximum susceptibility method, respectively, to perform LSP considering landslide types.
(4) Based on the frequency ratio accuracy, susceptibility index distribution pattern and prediction rate accuracy, uncertainty analysis of the LSP results considering landslide types is carried out again.

2.2. Analysis of instability characteristics of different types of landslides

The most common geological disasters in Huichang County are rock fall and colluvial landslides. According to the instability characteristics of landslides, for colluvial landslides, the rock and soil mass on the slope slide down along a certain weak surface or weak zone under the action of gravity for some reasons (Lombardo et al., 2021; Roberts et al., 2021); while for rock fall, the rock and soil on a steep slope suddenly break away from the parent body under the action of gravity, and then roll and/or accumulate at the foot of the slope (Li et al., 2020a, 2020b). The above two kinds of landslides are likely to evolve under similar geological structures and stratum lithology conditions. Meanwhile, they are generally connected to each other and sometimes even can be transformed into each other. Furthermore, rock fall products and deposits are often the important source of solid matter for colluvial landslides. The main differences between rock fall and colluvial landslides are described in Table 1.

In order to carry out the LSP model considering landslide types, a same set of 11 environmental factors is used to characterize the properties of rock fall and colluvial landslides in Huichang County. It is convenient for subsequent comparison and analysis of uncertainties in different types of landslide susceptibility based on the same set of environmental factors. However, the evolution and instability characteristics of different types of landslides show that the topography, land cover, hydrological environment and engineering geological conditions of areas where rock fall and colluvial landslides often occur are different (Sun et al., 2020b). Thus, it is necessary to reflect these differences in the LSP processes through correlation analysis.

The correlations between different types of landslides and environmental factors (not considering triggering factors) are

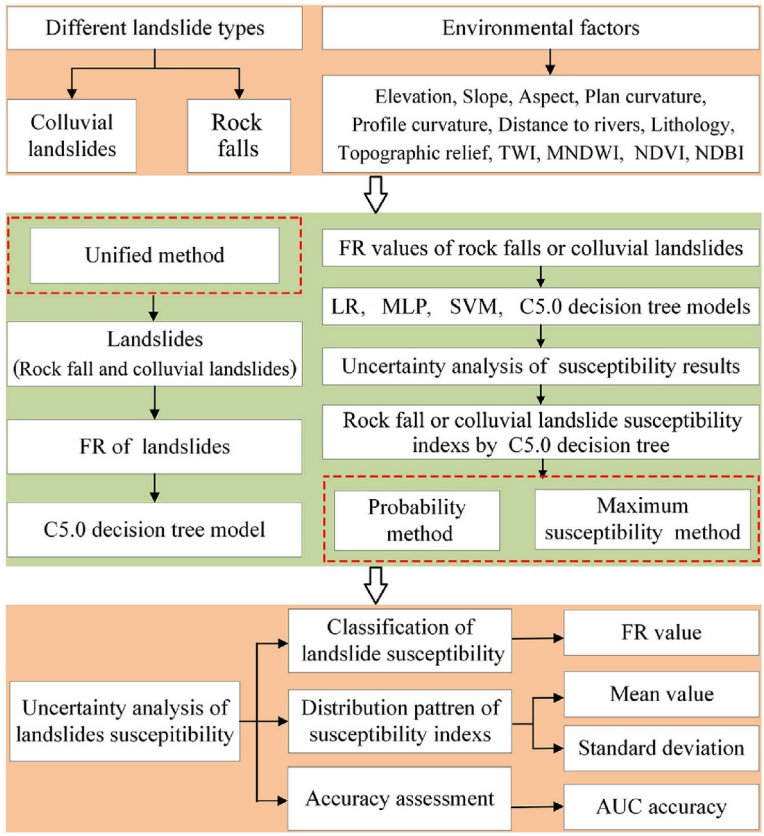

Fig. 1. Flow chart of LSP modeling.

important links between susceptibility indices and environmental factors. At present, many connection methods are proposed, such as weight of evidence, entropy index, information volume and frequency ratio and so on (Demir, 2019; Chang et al., 2020). Among them, frequency ratio method is very commonly used. For example, Wca and Shuai (2021) used frequency ratio to analyze the correlations between environmental factors and landslides, and predicted the landslide susceptibility in Muchuan County of China. Li et al. (2020a) and Bourenane and Bouhadad (2021) used frequency ratio method to predict the rock fall susceptibility. The frequency ratio method is also used in this study to characterize the correlations between rock fall, colluvial landslides and environmental factors. Then the calculated frequency ratios are considered as model input variables.

2.3. Coupled methods of LSP model considering landslide types

In this study, the unified method, probability method and maximum susceptibility method are innovatively proposed to predict the landslide susceptibility considering landslide types.

2.3.1. Unified method

Unified method does not distinguish the differences of the landslide characteristics and environmental factors of different types of landslides. This method directly couples different types of landslides as one type of landslide to calculate the connection values between landslides and environmental factors for LSP modeling. In this study, rock falls and colluvial landslides are coupled together to calculate their frequency ratios, which are used as the input variables of machine learning models. In the ArcGIS10.3 software, the scales of rock fall and colluvial landslides in Huichang County are mapped together (Fig. 2c).

2.3.2. Probability method

The probability method predicts the susceptibility indices of each type of landslide first, and then analyzes the probability statistical relationships between the susceptibility indices of different types of landslides. Finally, the final landslide susceptibility indices considering landslide types are calculated. In this study, the rock fall and colluvial landslides in Huichang County are used as examples to calculate the susceptibility indices by the probability method. The events of rock fall, colluvial landslides and landslides consider different types are set as R, L and G, respectively, then $P_R = P\{\text{Rock fall susceptibility index}\}$, $P_L = P\{\text{Colluvial landslide susceptibility index}\}$, $P_G = P\{\text{LSP index considering landslide types}\}$, and $P_G = P_L + P_R - P\{L \cup R\}$. The parameters ξ and η are adopted to indicate whether rock fall and colluvial landslides occur or not:

$$\xi = \begin{cases} 1 \text{ (rock fall occurs)} \\ 0 \text{ (rock fall does not occur)} \end{cases} \text{ and } P\{\xi = 1\} = P_L \tag{1}$$

$$\eta = \begin{cases} 1 \text{ (colluvial landslides occur)} \\ 0 \text{ (colluvial landslides do not occur)} \end{cases} \text{ and } P\{\eta = 1\} = P_R \tag{2}$$

Based on the following definition of correlation coefficient γ (Eq. (3)), and the relationships between $P\{L \cup R\}$, P_R and P_L, P_G can be calculated as

Table 1
The difference between rock fall and colluvial landslides.

Item	Rock fall	Colluvial landslides
Slope	Generally greater than 30°	Generally between 10° and 30°
Occurrence position	On the slope or above the slope foot	On the slope or at the slope foot
Boundary surface features	Side and bottom are independent of each other and cannot form a unified plane	Sometimes side and bottom can be connected into a unified plane or curved surface
Characteristics of bottom friction	High bottom surface friction	Low bottom surface friction
Geometry of the bottom surface	Rock fall block often exists independently	Each sliding is sometimes a uniform sliding surface
Movement essence	Crooked	Cut
Movement speed	Fast	Fast or slow
Movement state	Mostly rolling and jumping	Relative overall slip
Movement scale	Very small to large (block body generally does not exceed thousands of m^3)	Small or large
Typical sign	Reverse misalignment on the slope	Surface cracks, landslide perimeter, landslide tongue, etc.
Typical internal structure	Loose and cracked, partially overhead, imbricate structure	Original structures of rock formations are maintained, and shingled structures may also appear
Stacked body name	Dumped rocks	Landslide body

$$\gamma(\xi,\eta) = \frac{COV(\xi,\eta)}{D(\xi)D(\eta)} = \frac{E(\xi,\eta) - E(\xi)E(\eta)}{\sqrt{P_L(1-P_L)P_R(1-P_R)}} = \frac{P(L\cap R) - P_L P_R}{\sqrt{P_L(1-P_L)P_R(1-P_R)}} \tag{3}$$

$$P_G = P_L + P_R - \gamma\sqrt{P_L(1-P_L)P_R(1-P_R)} - P_L P_R \tag{4}$$

where E is the function of expectation, D is the function of standard deviation (SD), and COV is the function of correlation coefficient.

2.3.3. Maximum susceptibility method

The maximum susceptibility method is used to predict the susceptibility indices of different types of landslides in a certain grid unit, and then the predicted susceptibility indices are compared. Furthermore, the largest susceptibility index is set as the final landslide susceptibility index in this grid unit. In the specific modeling, the rock fall and colluvial landslide susceptibility maps are converted into special susceptibility indices and imported into the SPSS 24 software through "Raster to Point" tool in ArcGIS 10.3 software. Then, the susceptibility indices of rock fall and colluvial landslide in a same grid unit are compared by calculation of the variable operation in the SPSS 24 software. The index value is used as the landslide susceptibility index of this grid unit (Zhou et al., 2018). Finally, these landslide susceptibility indices are imported into ArcGIS 10.3 software again for susceptibility mapping and uncertainty analysis.

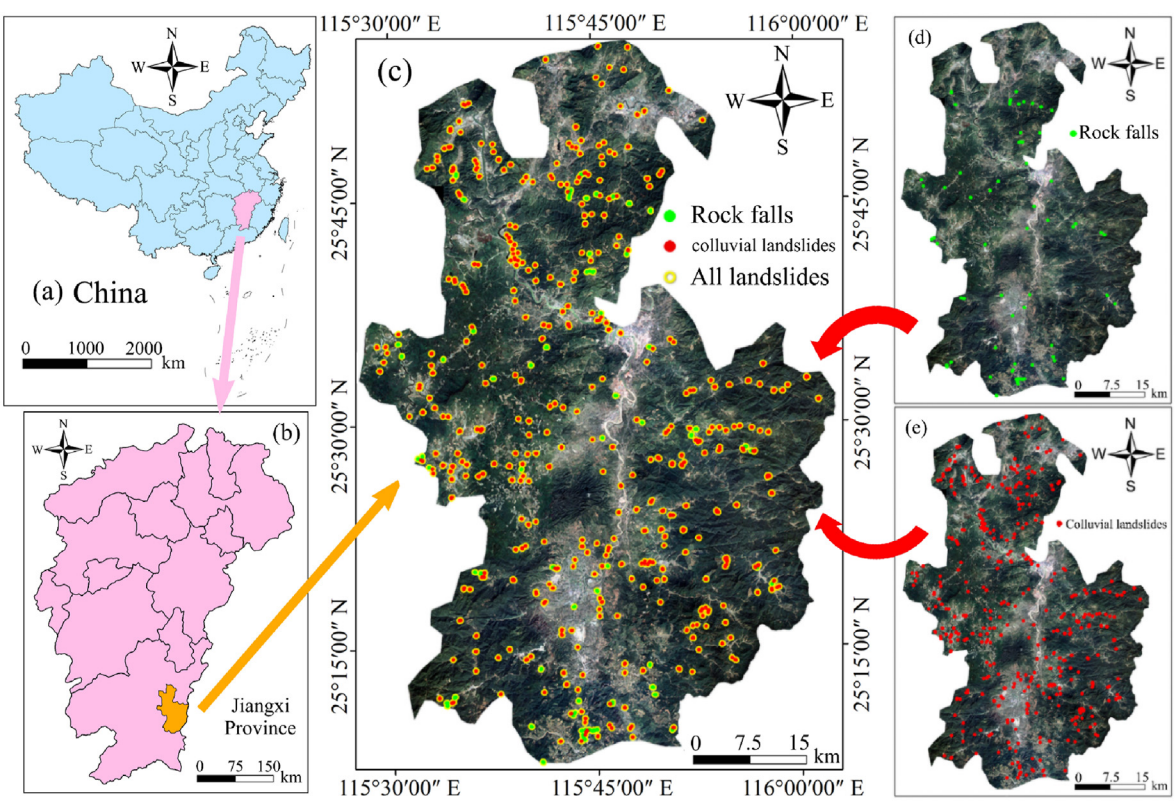

Fig. 2. Location of the study area and landslide and landslide surface obtained by the unified method.

2.4. Introduction of machine learning models

2.4.1. LR

The LR model is to form a multiple regression relationships between a dependent variable and multiple independent variables to predict the probability of an event (Cao et al., 2019). Landslide susceptibility predicted by LR equation is expressed as

$$y = \frac{e^{a_0+a_1x_1+a_2x_2+\cdots+a_nx_n}}{1+e^{a_0+a_1x_1+a_2x_2+\cdots+a_nx_n}} \tag{5}$$

where $x_i\ (i = 1, 2, \cdots, n)$ is the environmental factor; a_i is the contribution of each factor on landslide; a_0 is the regression intercept; and y is the probability of landslide occurrence.

2.4.2. MLP

The MLP is to randomly initialize the weight values between the input and hidden layers, and then use the activation function in the hidden layers to process the sum of the product of input layer and the weight during forward transfer process. The errors between output and expected values are calculated. Finally, during the error back propagation iterative process, the connection weights are continuously updated to obtain a result with the smallest error (Wang et al., 2020).

2.4.3. SVM

SVM is reasonable and effective in solving small sample, high-dimensional and nonlinear problems based on statistical learning theory (Huang and Zhao, 2018). This research is based on a set of linearly separable training vectors $\boldsymbol{x}_i\ (i = 1, 2, \cdots, n)$, and the training vectors include 11 environmental factors and corresponding output data $y_i = \pm 1$. The mathematical expression is $\|\omega\|^2/2$ and the constraint condition for correct classification is $y_i((\omega x_i)+b) \geq 1$. The Lagrange function is introduced to solve the convex quadratic optimization problem. In addition, radial basis function (RBF) is used as the kernel function (Zhang et al., 2022).

2.4.4. C5.0 decision tree

C5.0 decision tree has the advantages of easy understanding, simple modeling, high precision, and strong tolerance to data loss (Golkarian et al., 2018). The specific steps of this model are

(1) The information gain of all possible features is calculated for the node starting from the root node, and the feature with the largest information gain value is selected as the partitioning feature of the node.
(2) The child nodes from different values of the feature are created.
(3) The above steps are recursively called on the child nodes to build the decision tree.
(4) Until the information gain of all features is very small or there are no features to choose, the final decision tree is obtained.

2.5. Uncertainty analysis of LSP results

2.5.1. Distribution patterns of landslide susceptibility indices

The mean value and SD are important indicators reflecting the statistical pattern of landslide susceptibility indices (Huang et al., 2020a). Mean value and SD quantify the overall bias trend and the dispersion degree of susceptibility indices of landslides distributed in the study area, respectively. The large SD indicates that the landslide susceptibility indices have strong identifiability. In general, a greater SD and a smaller mean value indicate a lower LSP uncertainty under the condition of a higher prediction accuracy (Huang et al., 2020a).

2.5.2. Introduction of AUC accuracy

The AUC is a quantitative indicator to evaluate the overall accuracy of LSP modeling (Zhou et al., 2018). The idea of receiver operation characteristic curve is to first sort the samples in the test set, select different cutoff points in this order, and then predict the samples one by one as positive examples. Moreover, the "true positive rate" and "false positive rate" of current classifier calculated each time are respectively plotted as the vertical and horizontal axes of receiver operation characteristic curve. In general, the larger the AUC value, the better the LSP accuracy (Sun et al., 2020c).

2.5.3. Introduction of frequency ratio accuracy and prediction ratio accuracy

The frequency ratio accuracy is defined as the ratio of the sum of frequency ratios of high and very high susceptibility levels to the total frequency ratios. This method can be used to assess the accuracies of both supervised and non-supervised machine learning models (Huang et al., 2022a).

The prediction rate accuracy, which evaluates the goodness of fit between the landslide grid units and the predicted landslide susceptibility indices, is selected to conduct the susceptibility comparison of rock fall, colluvial landslides and landslides considering landslide types (Chung and Fabbri, 2008; Pradhan et al., 2010). Because the training/testing sample numbers of rock fall, colluvial landslides and landslides considering landslide types are different, it is difficult to use AUC accuracies to discuss the LSP uncertainty under different modeling conditions.

3. Study area and data sources

3.1. Introduction of Huichang County

Huichang County is located in the southeastern part of Jiangxi Province with a total area of about 2272.2 km^2 (Fig. 2). It is surrounded by high mountains, and low mountains are located in the middle, with a forest coverage of about 79%. This county belongs to a subtropical monsoon-type humid climate zone. The rainfall is concentrated and reaches about 752.9 mm from April to June. Huichang County is rich in water resources and the rivers have strong erosion effect on the reservoir bank slope. The geology belongs to a secondary structure of the New Cathaysia System and the main structures are folds and faults. The major strata are Cambrian, Jurassic and igneous rocks.

The type, location and scale of landslides are provided by the local Land and Resources Bureau through the landslide inventory mapping and field surveys (Nsengiyumva et al., 2019). Since 2016, two main types of landslides, namely rock fall and colluvial landslides, have been frequently reported in this county. The sliding mass of colluvial landslides are Quaternary residual and slope deposits with the relatively small slope of sliding surface and the motion model of clay/silt sliding. Meanwhile, most of rock falls can be characterized as moderately and/or highly weathered rock formation. The rock falls are dominated by vertical movement and relatively great slope. In terms of regional distribution, these landslides have the features of spatial clustering, relatively high temporal frequency and small scales (Korte and Shakoor, 2019). There are a total of 105 rock falls (Figs. 2d) and 350 colluvial landslides (Fig. 2e), both of which are mainly medium and small ones.

3.2. Environmental factors of rock fall and colluvial landslides

The environmental factors can be classified as the following categories: topography, land cover, hydrological and engineering geological factors (He et al., 2012). Combined with on-site geological survey, considering the difficulty in acquisition of relevant environmental factors and referring to the selection of landslide environmental factors in other related areas in Jiangxi Province, China, a total of 11 environmental factors are selected as input data of LSP model in this study (Chen et al., 2018; Hong et al., 2020; Huang et al., 2020b).

3.2.1. Topography factors

The topography factors include elevation, slope, profile curvature, plane curvature, topographic relief and terrain wetness index (TWI), which are all obtained from 30 m × 30 m DEM (Li et al., 2021). Taking elevation and slope as examples, the different elevations in Huichang County lead to the difference in the climate, vegetation and weathering degree of rocks in each area, further leading to different frequencies of landslides (Fig. 3a and Table 2). When the elevation ranges from 128 m to 316.8 m, the frequency ratio of colluvial landslides is greater than 1, indicating that the elevation ranging from 128 m to 316.8 m has an important influence on the occurrence of colluvial landslides. In addition, when the elevation ranges from 316.8 m to 485.6 m, the rock fall frequency ratio is greater than 1, indicating that rock fall is prone to occur in areas with an elevation of 316.8–485.6 m.

Slope plays an important role in landslide events (He et al., 2012). As shown in Fig. 3b and Table 2, when the slope is beyond 11.2°, the frequency ratio of rock fall is greater than 1, and there are 78.87% of the rock fall grid units in the interval. When the slope is in the range of 7.8°–22.4°, the frequency ratio of colluvial landslides is greater than 1, and colluvial landslide grid units in the interval account for 77.35%. This shows that the landslide mainly occurs within medium slope ranges.

3.2.2. Land cover and hydrological environment factors

Land cover is an important factor affecting the occurrence of landslides. For example, the normalized difference building index (NDBI) and normalized difference vegetation index (NDVI) reflect the influence of building distribution and vegetation on the evolution of landslides in the study area (Chen and Chen, 2021). NDVI reflects the relationship between landslides and surface vegetation density. As shown in Fig. 4a and Table 2, when NDVI is greater than 0.32, the probability of occurrence of colluvial landslides is greater; when NDVI is smaller than 0.32, the probability of occurrence of rock fall is greater.

The erosion of rivers on slope and the high soil water content will affect landslide evolution. The modified normalized difference water index (MNDWI) and distance to rivers are used to characterize the influence of hydrology on landslide evolution. Taking the distance to rivers shown in Fig. 4c and Table 2 as an example, 57%–60% of the grid units of rock fall and colluvial landslides are within 300 m from the river and the corresponding frequency ratios are greater than 1. It can be seen that the closer the distance to river, the higher the frequency of landslide occurrence.

3.2.3. Engineering geological factors

The scale and type characteristics of landslides in different strata lithologies are different (Zhao et al., 2020; Dai et al., 2021). Rock is an integral part of the slope body and the manifestation of the inherent physical properties of the landslide. As shown in Fig. 4d, the strata exposed in Huichang County are dominated by Cambrian and Jurassic rocks and the lithology mainly includes metamorphic, magmatic, carbonate and clastic rocks.

According to Table 2, under the condition of clastic rock, colluvial landslides have frequency ratios greater than 1, indicating that the occurrence probability of colluvial landslides is relatively high in clastic rock area and is relatively low in magmatic and metamorphic rock areas. Under the same condition, the rock fall has frequency ratios greater than 1, indicating that the probability of rock fall is relatively high in the clastic rock area and is relatively low in the magmatic and metamorphic rock areas. The distribution of carbonatite rocks in the study area is very small and the proportion of grid units in colluvial landslides is less than 2%. Rock fall does not occur in the carbonatite distribution area of Huichang County, hence, the distribution patterns of rock fall in the carbonatite areas cannot be drawn.

3.3. Preparation of modeling spatial data

Huichang County is divided into 3,001,146 grid units with 30 m × 30 m resolution, and two types of landslides, i.e. rock fall and colluvial landslides, are considered. First, the frequency ratios of the 11 environmental factors of rock fall and colluvial landslides are calculated and re-assigned as input variables of four machine learning models. Then the 105 rock falls are divided into 1432 grid units and the 350 colluvial landslides are divided into 5410 grid

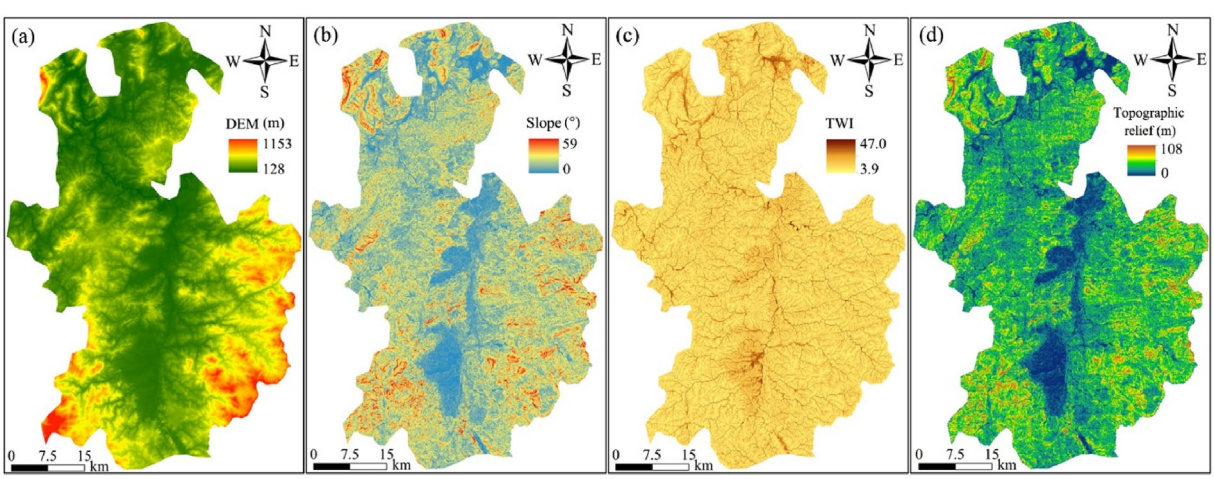

Fig. 3. Topographical factors: (a) DEM; (b) Slope; (c) Topographic relief; and (d) TWI.

Table 2
Frequency ratios of some typical environmental factors.

Environmental factor	Value	Percentage of raster grids (%)				Frequency ratios		
		Total areas	Rock fall	Colluvial landslides	Landslide	Rock fall	Colluvial landslides	Unified method
Elevation	128–240.5 m	26.06	22.05	31.74	30.89	0.846	1.218	1.185
	240.5–316.8 m	22.16	20.74	32.48	31.24	0.936	1.466	1.41
	316.8–397.2 m	18.53	23.75	13.91	15.07	1.282	0.75	0.813
	397.2–485.6 m	13.09	17.59	10.2	10.93	1.343	0.779	0.835
	485.6–582 m	8.77	5.12	7.42	6.83	0.584	0.846	0.779
	582–690.5 m	6.62	10.76	2.73	3.69	1.626	0.413	0.558
	690.5–831.1 m	3.48	0	1.52	1.35	0	0.438	0.387
	831.1–1152.5 m	1.29	0	0	0	0	0	0
Slope	0°–4.1°	16.75	0	2.9	2.21	0	0.173	0.132
	4.1°–7.8°	21.08	4.33	14.27	12.36	0.205	0.677	0.586
	7.8°–11.2°	20.44	15.49	24.04	23.01	0.758	1.176	1.126
	11.2°–14.6°	16.81	26.18	24.87	26.13	1.557	1.479	1.555
	14.6°–18.3°	12.11	20.77	18.74	19.91	1.715	1.548	1.644
	18.3°–22.4°	7.56	18.01	9.7	10.56	2.382	1.283	1.397
	22.4°–28.1°	4.07	10.91	3.66	4.19	2.681	0.899	1.029
	28.1°–58.2°	1.18	3.31	1.82	1.63	2.805	1.539	1.374
Topography relief	0–6.35 m	18.19	12.07	5.27	4.38	0.674	0.29	0.245
	6.4–11.9 m	25.24	27.95	22.7	20.26	1.112	0.9	0.806
	11.9–16.9 m	21.92	23.36	26.49	26.95	1.069	1.209	1.233
	16.9–22.5 m	16.64	17.72	23.94	24.76	1.067	1.439	1.491
	22.5–28.4 m	10.07	9.58	12.62	14.12	0.953	1.253	1.405
	28.4–35.2 m	5.38	7.35	6.34	6.08	1.369	1.18	1.132
	35.2–44.9 m	2.45	1.44	1.24	2.27	0.589	0.506	0.927
	44.9–108 m	0.62	0.53	1.41	1.19	0.847	2.268	1.914
TWI	3.91–6.61	32.53	36.35	44.32	39.31	1.285	1.362	1.39
	6.61–8.46	39.55	45.54	40.7	40.28	1.266	1.029	1.12
	8.46–11	17.44	15.49	11.54	15.18	0.793	0.662	0.777
	11–14.71	5.38	1.44	1.79	3.27	0.162	0.333	0.366
	14.71–25.35	1.72	0.39	0.93	1.1	0.086	0.54	0.241
	25.35–34.97	1.81	0.79	0.46	0.76	0.392	0.256	0.38
	34.97–38.52	1.26	0	0.18	0.1	0	0.145	0.15
	38.52–46.96	0.32	0	0.08	0	0	0.258	0
	0.37–0.51	0.64	0	0.05	0.03	0	0.077	0.045
NDVI	0–0.32	0.57	0.26	0.08	0.06	0.462	0.146	0.103
	0.32–0.48	1.42	1.05	1.21	1.25	0.738	0.85	0.875
	0.48–0.58	2.85	3.28	3.86	3.63	1.153	1.356	1.277
	0.58–0.65	6.75	9.45	10.88	10.74	1.399	1.611	1.59
	0.65–0.7	16.33	21.79	21.24	20.33	1.334	1.3	1.245
	0.7–0.75	26.83	23.1	27.88	28.02	0.861	1.039	1.044
	0.75–0.82	29.24	27.43	25.61	25.93	0.938	0.876	0.887
	0.82–1	16	13.65	9.24	10.05	0.853	0.577	0.628
Distance to rivers	<300 m	28.88	56.96	60.83	60.17	1.971	2.106	2.082
	300–600 m	24.64	11.81	19.49	18.59	0.478	0.791	0.752
	600–900 m	20.13	11.81	9.59	9.77	0.587	0.476	0.486
	>900 m	26.35	19.42	10.51	11.47	0.74	0.399	0.437
Lithology	Clastic	33.73	56.96	41.11	40.5	1.971	1.222	1.204
	Magmatic	34.35	11.81	1.64	31.99	0.478	0.048	0.933
	Metamorphic	30.16	11.81	26.29	26.07	0.587	0.874	0.867
	Carbonatite	1.76	19.42	30.96	1.44	0.74	17.717	0.821

units (all are assigned a value of 1). At the same time, non-rock fall and non-colluvial landslide grid units with the same number of rock fall and colluvial landslide grid units are randomly selected in non-disasters areas (all are assigned a value of 0). These two sets of data are merged as the output variables of four machine learning models. Next, according to the 70%: 30% random division, the model training and testing sets are obtained and the cross-validation method is used to realize their effective verification (Sun et al., 2020c). Furthermore, the frequency ratios of all grid units in the study area are substituted into the four trained machine learning models to calculate the susceptibility of rock fall and colluvial landslide in Huichang County (Hong et al., 2020). Finally, the obtained results are imported into the ArcGIS10.3 software to prepare the susceptibility maps of rock fall and colluvial landslide.

Unified method of the LSP model also requires the preparation of spatial data sets, which is similar to the preparation of spatial data sets for the susceptibility prediction of rock fall and colluvial landslide. After rock fall and colluvial landslide are directly coupled into landslide by the unified method, a total of 455 landslides without considering landslide types have been prepared, which can be divided into 6842 landslide grid units. Then the frequency ratios of environmental factors are calculated after the input variables are obtained. Finally, the input variables are substituted into the four trained machine learning models to calculate the landslide susceptibility indices in all grid units in the study area. In addition, since the other two LSPs are carried out on the basis of the susceptibility indices of rock fall and colluvial landslide, there is no need to recalculate the frequency ratios and prepare related spatial data sets.

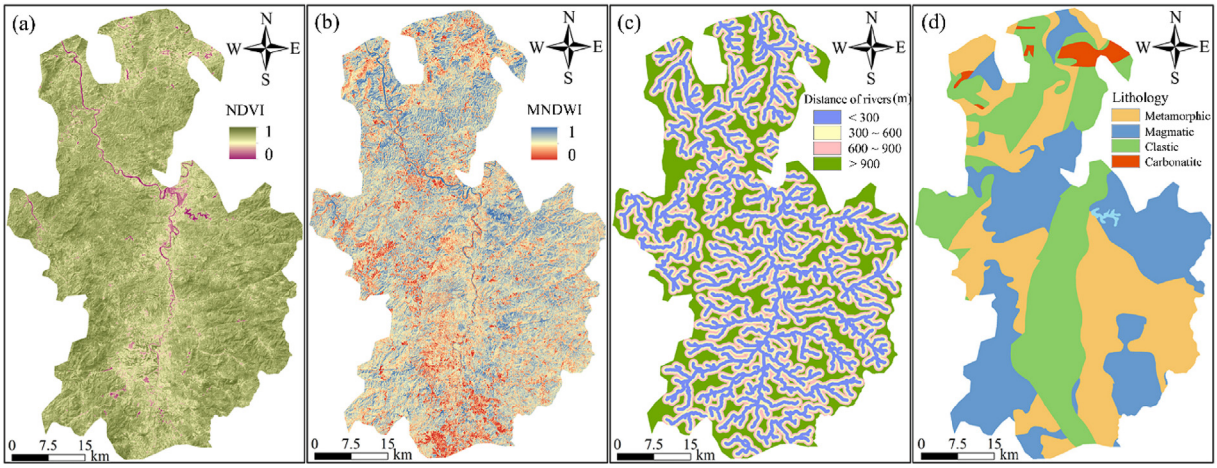

Fig. 4. Land cover, hydrology and geological factors: (a) NDVI; (b) MNDWI; (c) Distance to rivers; and (d) Litholog.

4. Results of single rock fall/colluvial landslide susceptibility prediction

4.1. Collinearity diagnosis of environmental factors

If there is a high degree of correlation between these environmental factors, the model estimation may be distorted or difficult to build models accurately. Therefore, it is necessary to perform multi-collinearity diagnosis. The collinearity is judged by counting the variance inflation factors (VIFs) and tolerance values of the 11 environmental factors. When the VIF is greater than or equal to 10, or the tolerance is less than or equal to 0.2, the collinearity between the environmental factors is relatively serious (Kalantar et al., 2019; Merghadi et al., 2020; Huang et al., 2022b). It can be seen from Table 3 that the maximum value of VIFs of rock fall is 1.496 and the minimum value of tolerance is 0.669, and the maximum value of VIF of colluvial landslide is 2.585 and the minimum tolerance is 0.387. Therefore, there is no serious multi-collinearity among the environmental factors of both rock fall and colluvial landslide. All the 11 environmental factors can be used to predict the susceptibility of rock fall and colluvial landslides in the study area.

4.2. Rock fall susceptibility prediction by various models

4.2.1. LR model for rock fall susceptibility prediction

The LR model is trained and tested on the basis of the rock fall spatial data set. The related regression coefficients (β), standard errors and significances of the 11 environmental factors are calculated. The calculation results show that the significances of all environmental factors are less than 0.05, indicating that each variable is statistically significant. Meanwhile, the β values of all environmental factors are positive, showing that these factors promote the occurrence of rock fall. The coefficients of elevation, slope, plane curvature, profile curvature, topography relief, TWI, NDVI, NDBI, MNDWI, distance to rivers and lithology are 1.341, 1.262, 0.566, 0.76, 1.121, 1.412, 0.415, 1.463, 1.432, 1.643 and 0.196, respectively, with a intercept value of −14.877. These regression coefficients and Eq. (5) are used to predict rock fall susceptibility indices.

Common methods for classifying susceptibility levels include quantile method, natural break point method and equal intervals method (Ayalew and Yamagishi, 2005). In this study, all predicted landslide susceptibility indices are divided into five levels: very low, low, medium, high and very high levels using the natural break point method. Finally, the rock fall susceptibility predicted by the LR model is mapped, as shown in Fig. 5a.

Table 3
Multiple linear regression coefficients and constant terms.

Environmental factors	Rock fall		Colluvial landslides	
	Tolerance	VIF	Tolerance	VIF
Elevation	0.925	1.082	0.854	1.171
Slope	0.669	1.496	0.418	2.39
Plane curvature	0.809	1.236	0.819	1.22
Profile curvature	0.966	1.035	0.992	1.008
Topography relief	0.872	1.147	0.473	2.112
TWI	0.795	1.258	0.775	1.29
NDVI	0.689	1.452	0.446	2.24
NDBI	0.675	1.482	0.387	2.585
MNDWI	0.924	1.082	0.804	1.243
Distance to rivers	0.896	1.116	0.832	1.202
Lithology	0.853	1.173	0.959	1.043

4.2.2. MLP model for rock fall susceptibility prediction

In SPSS 24 software, a MLP model with input, output and hidden layers is constructed based on the frequency ratio values of 11 environmental factors as inputs and with the rock fall inventory data as outputs. In the process of MLP modeling, the learning rate, momentum and iteration time are set to 0.01, 0.3 and 2000, respectively. Meanwhile, the number of hidden layers is set to 2 and the activation function is the Softmax function. Finally, the trained MLP is used to predict the rock fall susceptibility index of each grid unit in the study area with susceptibility map shown in Fig. 5b.

4.2.3. SVM model for rock fall susceptibility prediction

In the modeling process of SVM model, the global search method (Kong et al., 2021) is used to determine the rule parameter (C), regression accuracy and kernel parameter (γ) of SVM to be 6, 0.1 and 0.09, respectively. The stopping criterion of SVM is set to 10^{-3} and the remaining parameters are set as default values. Then the trained SVM is used to predict the rock fall susceptibility index of each grid unit in the study area, and the susceptibility map is drawn in Fig. 5c.

4.2.4. C5.0 decision tree for rock fall susceptibility prediction

C5.0 decision tree model is realized in the SPSS Modeler18.0 software for rock fall susceptibility prediction. The decision tree is used as the output type and the boosting method is used to

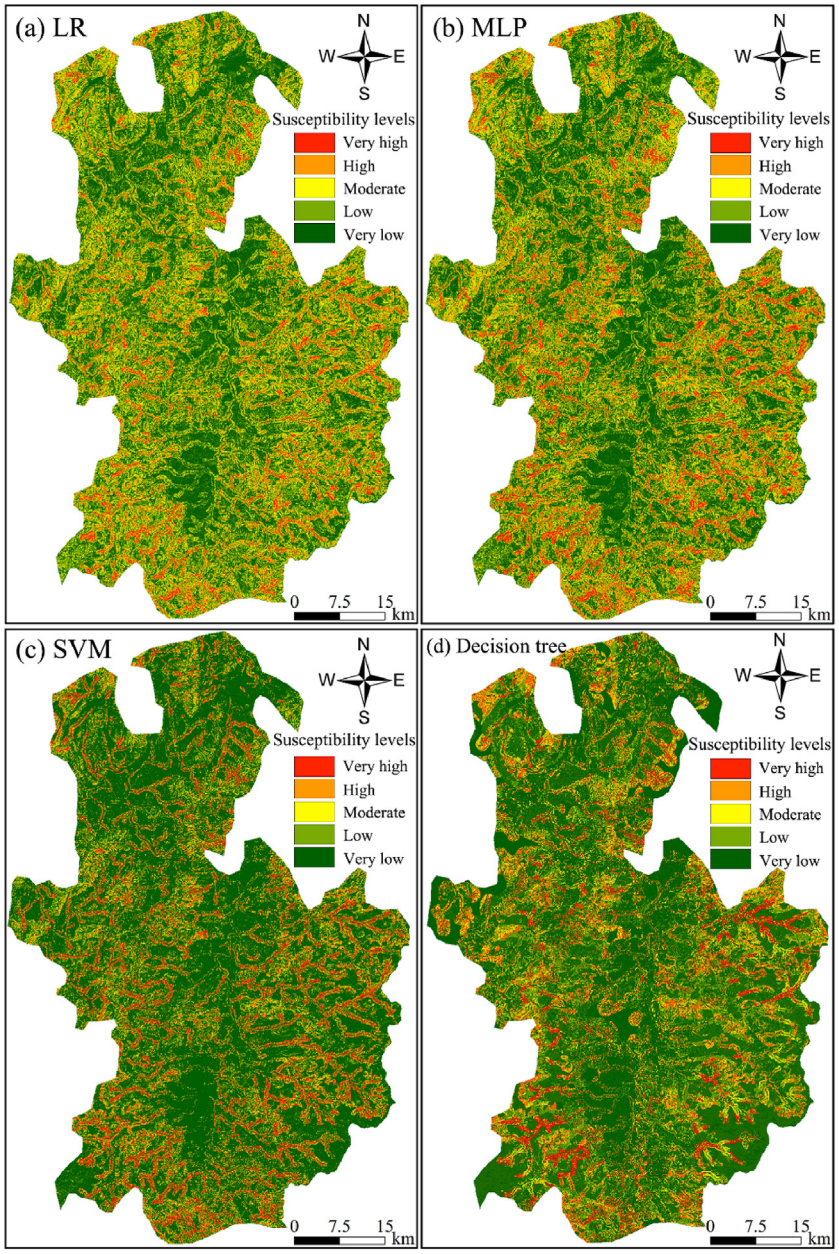

Fig. 5. Rock fall susceptibility maps predicted by (a) LR, (b) MLP, (c) SVM, and (d) C5.0 decision tree models.

improve the accuracy of the model. At the same time, the cross-validation method is used to estimate the accuracy of the C5.0 decision tree model and the remaining parameters take default values to avoid model overfitting (Guo et al., 2021). Finally, this trained model is used to predict the rock fall susceptibility indices of the study area (Fig. 5d).

4.3. Colluvial landslide susceptibility prediction by various models

4.3.1. LR model for colluvial landslide susceptibility prediction

The training/testing data of colluvial landslide are imported into SPSS 24 software to obtain the regression coefficient (β), standard error and significance of each environmental factor of the LR equation. The LR modeling results show that the significances of all environmental factors are less than 0.05, indicating that each variable is statistically significant. The coefficients of elevation, slope, plane curvature, profile curvature, topography relief, TWI, NDVI, NDBI, MNDWI, distance to rivers and lithology are 0.91, 1.381, 0.812, 0.777, 0.33, 0.623, 0.403, 1.112, 0.687, 0.95 and 0.433, respectively, with a intercept value of −10.025. Therefore, these environmental factors contribute to the evolution of colluvial landslide. Furthermore, the slope and NDBI have greater impacts on the evolution of colluvial landslide and their values are all greater than 1. The trained logistic regression coefficients and Eq. (5) are applied to calculate the colluvial landslide susceptibility indices, and corresponding susceptibility map is drawn in Fig. 6a.

4.3.2. MLP model for colluvial landslide susceptibility prediction

In the SPSS 24 software, the colluvial landslide training/testing data are used. The Softmax function is selected as the activation function, the number of hidden layers is set to 2, and each layer contains 6 nodes when constructing MLP model. In addition, the learning rate, momentum and iteration time are set to 0.01, 0.35 and 2000, respectively. Then the trained MLP model is used to

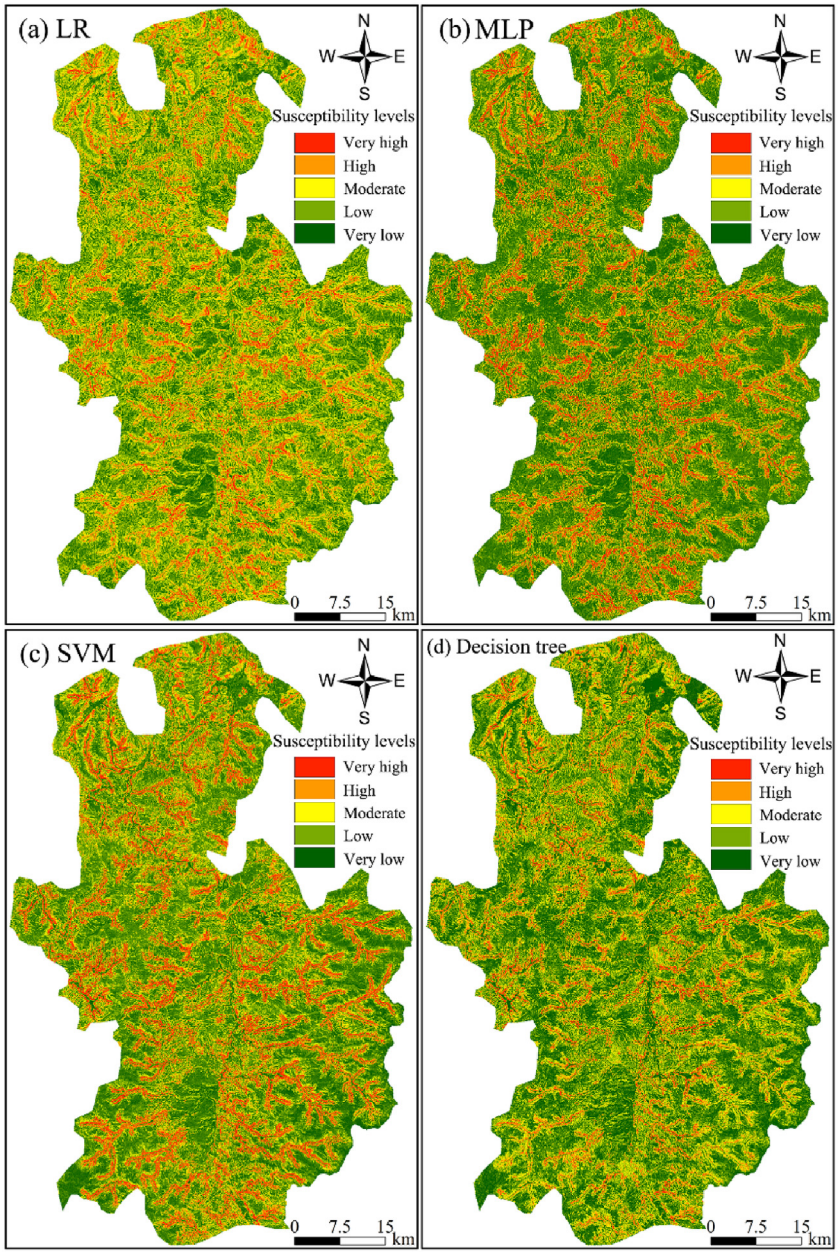

Fig. 6. Colluvial landslide susceptibility maps predicted by (a) LR, (b) MLP, (c) SVM, and (d) C5.0 decision tree models.

predict the colluvial susceptibility indices, and the colluvial landslide susceptibility is mapped in Fig. 6b.

4.3.3. SVM model for colluvial landslide susceptibility prediction

In the SVM model, the linearly inseparable data are mapped into a high-dimensional feature space to make these training and testing samples linearly separable. The stopping criterion, rule parameter (C), regression accuracy and kernel parameter (γ) of the SVM model are set to 10^{-3}, 5, 0.1 and 0.09, respectively. Finally, the trained SVM model is used to predict the colluvial landslide susceptibility in the Huichang County (Fig. 6c).

4.3.4. C5.0 decision tree for colluvial landslide susceptibility prediction

In the C5.0 decision tree model, the cross-validation method is also applied to ensure the model accuracy. During the modeling process, the expert mode is selected for decision tree pruning. The pruning severity is set to 80, the minimum number of records for each sub-branch is set to 15, the global pruning is adopted, and the remaining parameters are set to default. Finally, the trained C5.0 decision tree is used to predict and map the colluvial landslide susceptibility indices (Fig. 6d).

4.4. Uncertainty analysis of single rock fall/colluvial landslide susceptibility results

4.4.1. Frequency ratio accuracy

Based on a certain type of landslide susceptibility map, the number of landslide grid units and the total number of grid units are selected at all susceptibility levels (very high, high, moderate, low and very low levels). Then, the frequency ratio value of each level is calculated by Eq. (3), and the distribution patterns of

frequency ratio values of all levels of rock fall and colluvial landslides are respectively discussed under each machine learning model (Table 4). A comparative analysis of the four models finds that the frequency ratios of rock fall and colluvial landslide susceptibility gradually decrease from very high to very low levels.

The calculation results show that the frequency ratio accuracies of the C5.0 decision tree model for rock fall and colluvial landslide susceptibility are the largest (86.17% and 95.84%, respectively), followed by SVM (80.34% and 81.64%), MLP (85.26% and 79.37%), and LR (84.68% and 84.51%). In summary, it is found that the accuracies of rock fall and colluvial landslide susceptibility maps under the C5.0 decision tree model are higher than the others.

4.4.2. AUC accuracy

Evaluation of model quality is one of the key steps in LSP modeling. The AUC is widely used to quantitatively evaluate the performance of LSP models (Hong et al., 2020). The *X*-axis of the receiver operating characteristic curve indicates the proportion of non-landslides that are correctly classified, and the *Y*-axis indicates the proportion of landslides that are correctly classified (Cantarino et al., 2018). The AUC results are shown in Fig. 7, which suggest that the LR, MLP, SVM and C5.0 decision tree models have good predictive capabilities for rock fall and colluvial landslide on the whole. In particular, the AUC values for predicting rock falls in various models exceed 88.3%. The four models have different efficiencies in colluvial landslide susceptibility prediction, that is, the accuracies of LR (AUC = 80.6%) and MLP (AUC = 80.4%) are not outstanding, the SVM (AUC = 82.6%) has a better accuracy, and the C5.0 decision tree (AUC = 94.2%) model has the best accuracy. To sum up, the C5.0 decision tree has the highest prediction performance for different types of landslide susceptibility, followed by the SVM, LR and MLP models.

Table 4
Rock fall and colluvial landslide susceptibility frequency ratios of each level.

Landslide type	Class	Frequency ratios of LSP class			
		LR	MLP	SVM	C5.0
Rock fall	Very low	0.043	0.036	0.064	0.034
	Low	0.193	0.25	0.398	0.222
	Moderate	1.021	0.889	1.213	1.221
	High	1.751	1.64	1.51	3.323
	Very high	5.196	5.156	5.337	5.882
Colluvial landslides	Very low	0.135	0.168	0.101	0.011
	Low	0.279	0.407	0.301	0.087
	Moderate	0.696	0.893	0.752	0.296
	High	1.814	1.69	1.383	1.755
	Very high	4.244	3.957	3.747	7.341

4.4.3. Susceptibility index distribution patterns

In this paper, the mean value and SD are used to reflect the average level and dispersion degree of the susceptibility index distribution patterns of rock fall and colluvial landslides, so as to analyze the uncertainties of rock fall and colluvial landslide susceptibility prediction modeling. The calculation results are shown in Table 5 and Fig. 8a–d. It can be seen from Table 5 and Fig. 8a–d that the mean value ranking of the rock fall susceptibility indices measured by the four machine learning models is $\text{Mean}_{(LR)} > \text{Mean}_{(MLP)} > \text{Mean}_{(C5.0\ decision\ tree)} > \text{Mean}_{(SVM)}$, and the corresponding SD ranking is $\text{SD}_{(MLP)} > \text{SD}_{(LR)} > \text{SD}_{(SVM)} > \text{SD}_{(C5.0\ decision\ tree)}$.

These comparisons show that: (1) The mean value of rock fall susceptibility indices predicted by the SVM is the smallest, the SD is medium, and the frequency ratio accuracy and AUC accuracy are unsatisfied; (2) Both the mean value and SD of rock fall susceptibility indices predicted by the C5.0 decision tree are relatively small with the highest frequency ratio accuracy and AUC accuracy, and the distribution patterns of the predicted rock fall susceptibility indices are in line with actual landslide distribution; (3) Both the mean value and SD of rock fall susceptibility indices predicted by the MLP are relatively large, indicating that the rock fall susceptibility indices are not concentrated in the very low and low susceptibility levels.

The mean value ranking of the colluvial landslide susceptibility indices predicted by the four machine learning models (Table 5 and Fig. 8e–h) is $\text{Mean}_{(LR)} > \text{Mean}_{(SVM)} > \text{Mean}_{(MLP)} > \text{Mean}_{(C5.0\ decision\ tree)}$, and the corresponding SD ranking is $\text{SD}_{(SVM)} > \text{SD}_{(MLP)} > \text{SD}_{(C5.0\ decision\ tree)} > \text{SD}_{(LR)}$. These comparisons indicate that the mean value and SD of colluvial landslide susceptibility indices predicted by the C5.0 decision tree models are small with satisfied LSP accuracy, while those predicted by the SVM, LR and MLP models are almost the opposite. In summary, the C5.0 decision tree model can better distinguish different types of landslide susceptibility indices and well reflect the difference of susceptibility indices in various grid units.

5. Results of LSP considering landslide types using C5.0 decision tree

5.1. LSP considering landslide types

Based on the comprehensive analysis of Section 4, we obtain several rules from the susceptibility prediction of rock fall and colluvial landslide: (1) Comparing the frequency ratio values of all susceptibility levels, the frequency ratio of rock fall and colluvial landslide gradually decreases from very high to very low susceptibility levels. (2) According to the analysis of the mean and SD of

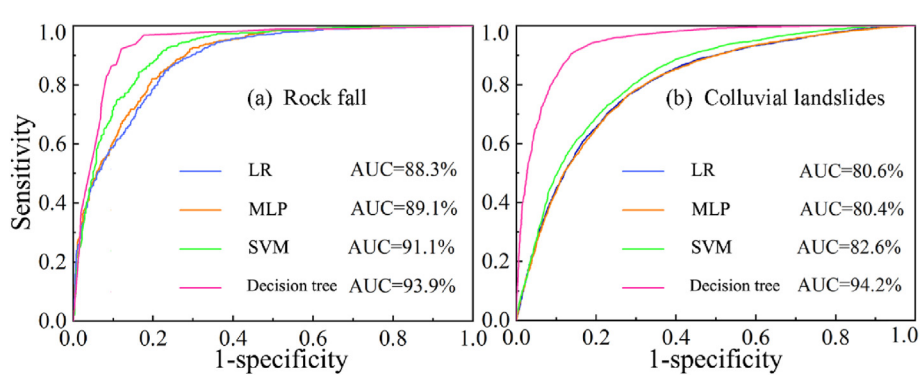

Fig. 7. AUC accuracies of (a) single rock fall and (b) colluvial landslide susceptibility prediction.

Table 5
Mean value and SD of rock fall and colluvial landslide susceptibility indices.

Coupled models	Rock fall			Colluvial landslides		
	Mean	SD	AUC accuracy (%)	Mean	SD	AUC accuracy (%)
LR	0.361	0.282	88.3	0.361	0.231	80.6
MLP	0.317	0.297	89.1	0.336	0.241	80.4
SVM	0.278	0.277	91.1	0.34	0.256	82.6
C5.0	0.281	0.275	93.9	0.297	0.239	94.2

the susceptibility indices of different models, the rock fall and colluvial landslides susceptibility indices are concentrated in the very low and low susceptibility levels. (3) Among the four models, the C5.0 decision tree model has a lower uncertainty of the susceptibility prediction, followed by the SVM, MLP and LR models. In summary, the C5.0 decision tree is selected to model the LSP considering landslide types due to its efficient performance. Meanwhile, the boosting method is used to improve its accuracy, and the cross-validation method is also used to ensure its accuracy.

5.1.1. Unified method to LSP

The unified method firstly combines the rock fall surfaces and colluvial landslide surfaces in Huichang County into new landslide surfaces through ArcGIS 10.2 software. Then the new frequency ratios based on the new landslide surface are calculated as the input variables of the C5.0 decision tree model. That is to say, the landslide susceptibility considering landslide types is predicted by the C5.0 decision tree model in the SPSS Modeler 18.0 software. For this model building, the expert mode is selected for global pruning of the decision tree, the pruning severity is set to 80, the minimum number of records for each sub-branch is set to 15, and the other parameters are set as default values. The final landslide susceptibility map produced is shown in Fig. 9a.

5.1.2. Probability method to LSP

For the probability method, the rock fall and colluvial landslide susceptibility indices predicted by the C5.0 decision tree model are first imported into the SPSS 24 software. Then the Pearson correlation coefficient (γ) is calculated through correlation analysis as

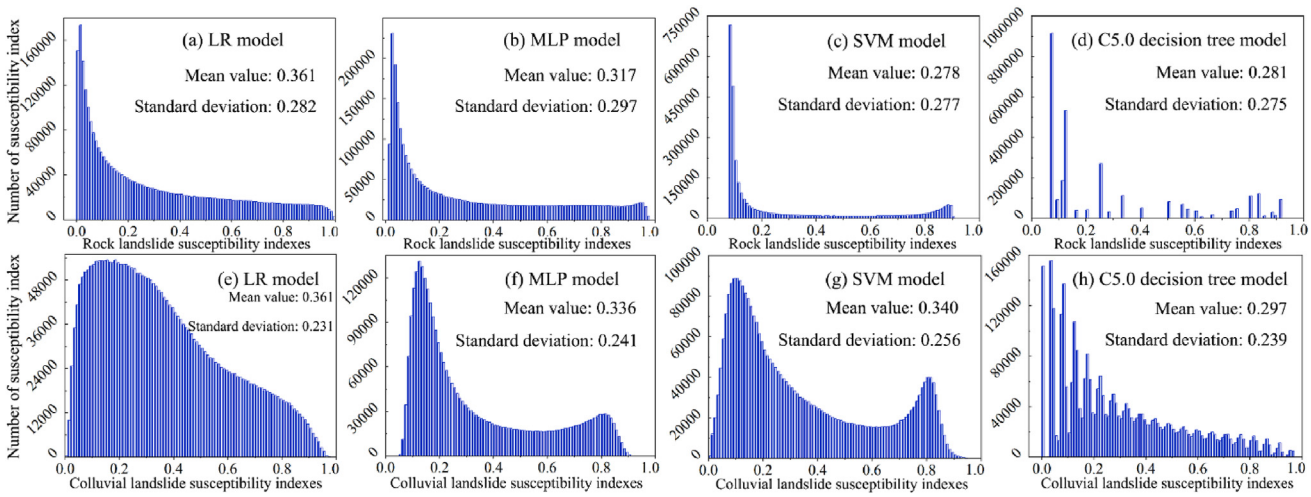

Fig. 8. Mean value and SD of rock fall and colluvial landslide susceptibility indices predicted by the LR, MLP, SVM, and C5.0 decision tree models.

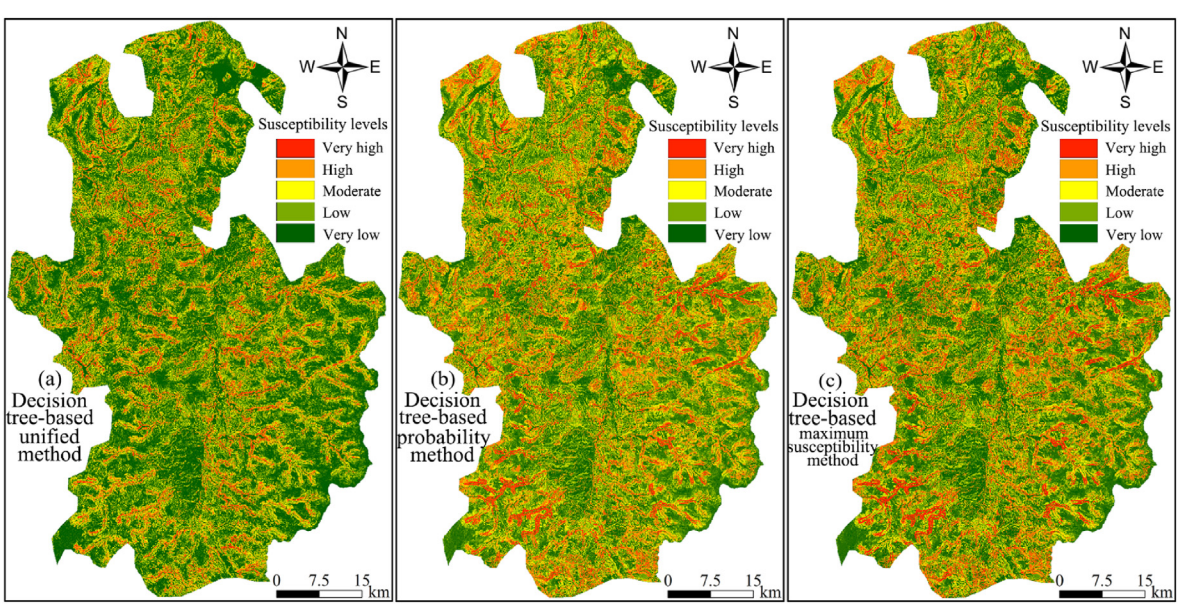

Fig. 9. Landslide susceptibility maps predicted by the C5.0 decision tree model based (a) unified method, (b) probability method and (c) maximum susceptibility method.

$\gamma = 0.426$. According to Eq. (4), the probability coupled calculations of rock fall susceptibility indices (P_R) by the C5.0 decision tree model, colluvial landslide susceptibility indices (P_L) by C5.0 decision tree model and correlation coefficient (γ) are carried out. Finally, the landslide susceptibility indices (P_G) are obtained and mapped in ArcGIS 10.2 software (Fig. 9b).

5.1.3. Maximum susceptibility method to LSP

The maximum susceptibility method also needs to first import rock fall and colluvial landslide susceptibility indices predicted by the C5.0 decision tree model into the SPSS 24 software. Then, by using the if-conditional statement in the variable option, the rock fall and colluvial landslide susceptibility indices predicted by the C5.0 decision tree model in the same grid unit are compared. Finally, the larger susceptibility index value of the two is selected as the final landslide susceptibility index and the mapping management is carried out (Fig. 9c).

5.2. Uncertainty analysis of LSP considering landslide types

5.2.1. Results of frequency ratio accuracy analysis

Comparing the frequency ratios of the C5.0 decision tree based unified method, probability method and maximum susceptibility method, it is found that the frequency ratios decrease from very high to very low susceptibility levels considering landslide types (Table 6). This comparison indicates that the landslide susceptibility indices are concentrated in the very low and low susceptibility levels, and the distribution in other susceptibility levels gradually decreases. It is also found from Table 6 that the frequency ratio accuracy of unified method is the largest (94.44%), followed by the probability method (88.65%) and the maximum susceptibility method (88.45%). These comparisons indicate that the C5.0 decision tree based unified method has predicted landslide susceptibility reliably and efficiently.

5.2.2. Comparison analysis of AUC

The AUC values are used to compare the LSP accuracies considering landslide types. It can be seen from Fig. 10 that the C5.0 decision tree based unified method (AUC = 90.8%) has significantly higher LSP performance than the C5.0 decision tree based probability method (AUC = 86%) and the maximum susceptibility method (AUC = 85.6%). This also shows that the LSP performance of the probability method and the maximum susceptibility method is relatively close and is quite different compared with the unified method. Anyway, the AUC values of the three methods are all greater than 85%, indicating that these methods all have a good predictive ability for LSP considering landslide types.

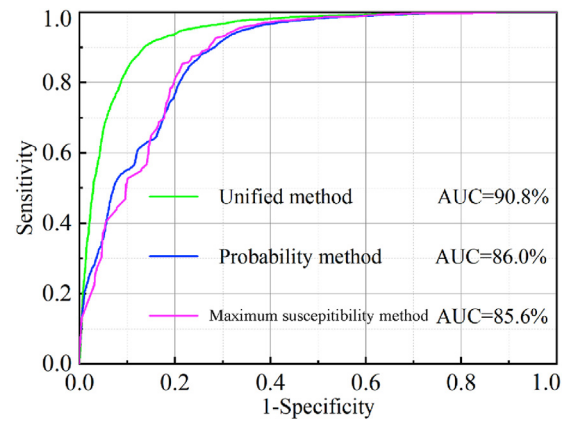

Fig. 10. The AUC accuracy of LSP by C5.0 decision tree model.

5.2.3. Distribution patterns of landslide susceptibility indices considering landslide types

Fig. 11 shows that the three coupled methods considering landslide types can distinguish the landslide susceptibility indices well and reflect the difference of the susceptibility indices in different grid units well, due to their relatively small mean values and relatively large SDs. However, a further comparison of these two indictors suggests that the mean value ranking of the landslide susceptibility indices predicted by the C5.0 decision tree considering landslide types is $\text{Mean}_{(\text{Probability method})} > \text{Mean}_{(\text{Maximum susceptibility method})} > \text{Mean}_{(\text{Unified method})}$, and the SD ranking of is $\text{SD}_{(\text{Maximum susceptibility method})} > \text{SD}_{(\text{Unified method})} > \text{SD}_{(\text{Probability method})}$. A smaller mean value and a higher SD indicate a superior LSP performance and a lower uncertainty of unified method when considering landslide types (Fig. 11).

6. Discussion

6.1. Comparisons of machine learning models for LSP considering landslide types

This paper uses LR, MLP and SVM models to predict LSP considering landslide types, and the results are compared with those predicted by the C5.0 decision tree, so as to avoid

Table 6
Frequency ratios of LSP predicted by the C5.0 decision tree model.

C5.0 decision tree based method	Class	Grid number in the study area	Percentage of grids in study area (%)	Landslide grid number	Percentage of landslide grids (%)	Frequency ratio
Unified method	Very low	1,153,118	38.1	55	0.8	0.021
	Low	736,115	24.4	173	2.5	0.103
	Moderate	512,371	17.1	547	8.1	0.469
	High	364,912	12.6	1905	27.9	2.295
	Very high	234,630	7.8	4147	60.7	7.77
Probability method	Very low	950,333	31.7	42	0.6	0.019
	Low	773,612	25.8	200	2.9	0.114
	Moderate	492,796	16.4	767	11.2	0.684
	High	366,702	12.2	1774	26.1	2.127
	Very high	417,703	13.9	4044	59.2	4.256
Maximum susceptibility method	Very low	1,015,927	33.9	45	0.7	0.019
	Low	775,345	25.8	220	3.2	0.125
	Moderate	486,197	16.2	814	11.9	0.736
	High	249,495	8.3	1691	24.8	2.979
	Very high	474,182	15.8	4057	59.5	3.761

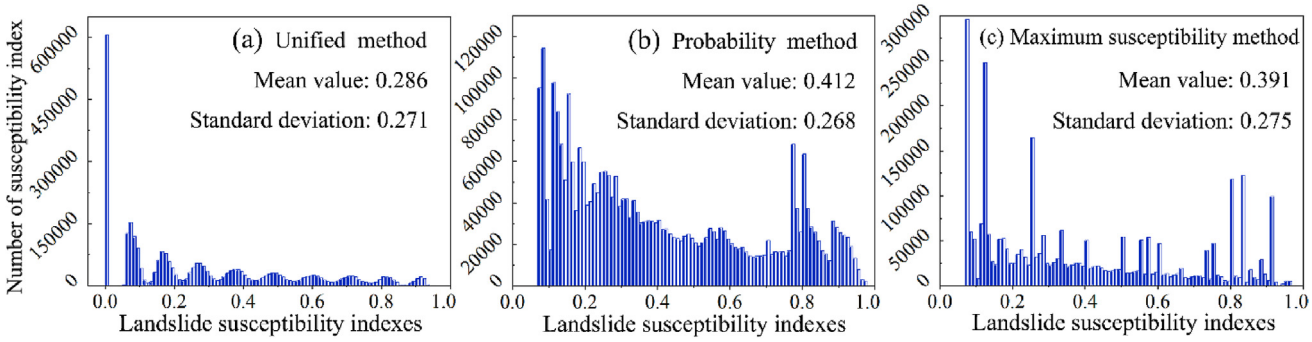

Fig. 11. Mean value and SD of landslide susceptibility indices predicted by the C5.0 decision tree based (a) unified method, (b) probability method, and (c) maximum susceptibility method.

uncertainties caused by different machine learning models (Huang et al., 2020a).

6.1.1. LSP considering landslide types based on LR, MLP and SVM models

In the process of unified method for LSP considering landslide types, the model parameters are set as follows.

(1) For the LR model, the β values of environmental factors are all positive numbers, showing that these environmental factors promote the evolution of landslides.
(2) The MLP model chooses the Softmax function as the activation function with 2 hidden layers, and each layer contains 6 nodes. The learning rate, momentum, and iteration time are set to 0.01, 0.35 and 2000, respectively.
(3) The SVM model selects RBF as the kernel function and sets the stopping criterion, rule parameter (C), regression accuracy and kernel parameter (γ) to 10^{-3}, 5, 0.1 and 0.09, respectively.

The probability method calculates the Pearson correlation coefficients between rock fall and colluvial landslide susceptibility indices in the LR, MLP and SVM models, which are 0.677, 0.605 and 0.594, respectively. Then, according to Eq. (4), the rock fall susceptibility index (P_R), colluvial landslide susceptibility index (P_L), and Pearson correlation coefficients are probabilistically coupled to calculate the final landslide susceptibility index (P_G).

The maximum susceptibility method uses the "if-conditional statement" to select the larger susceptibility index between the rock fall and colluvial landslide susceptibility indices as the final landslide susceptibility index. Finally, all the landslide susceptibility considering landslide types predicted by the LR, MLP and SVM models are mapped in ArcGIS 10.2 software. In order to save space, Fig. 12 only shows landslide susceptibility maps predicted by the LR, MLP and SVM based unified method.

6.1.2. Comparations of decision tree, LR, MLP and SVM models considering landslide types

The susceptibility results of LR, MLP and SVM models well reflect the differences in susceptibility indices between different grid units. This is because we can use less high susceptibility indices to reflect more known landslide locations. Taking the LR model as an example (Table 7), the mean value ranking of the three types of landslide susceptibility indices is $\text{Mean}_{(\text{Maximum susceptibility method})} > \text{Mean}_{(\text{Probability method}} > \text{Mean}_{(\text{Unified method})}$. The corresponding SD ranking is $\text{SD}_{(\text{Maximum susceptibility method})} > \text{SD}_{(\text{Probability}}$

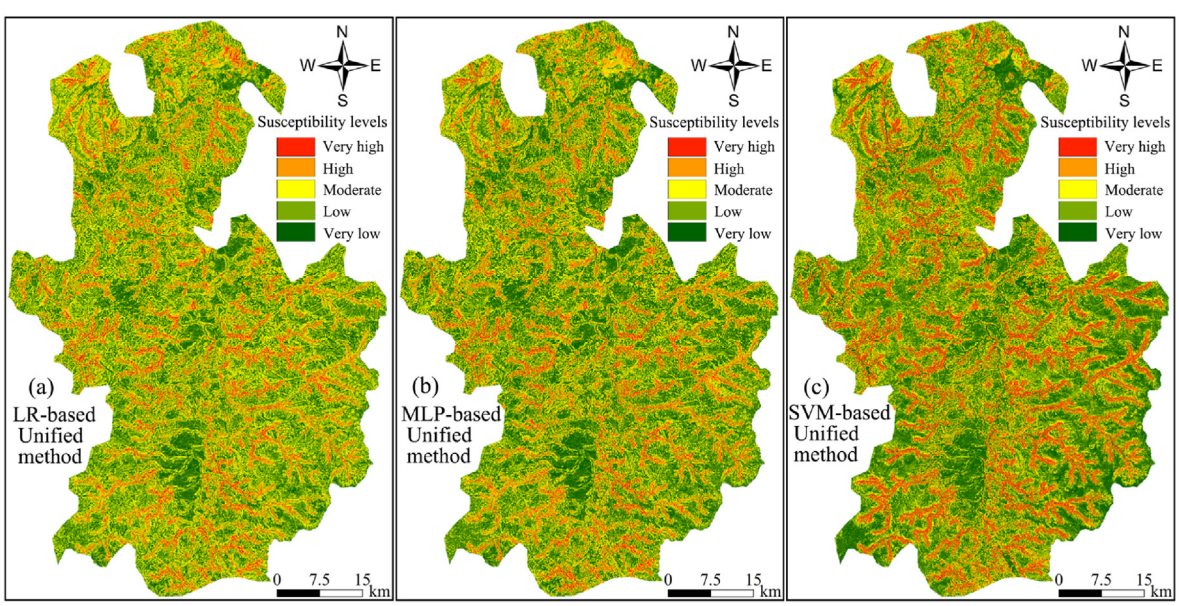

Fig. 12. Landslide susceptibility maps predicted by (a) LR,(b) MLP and (c) SVM based unified method.

Table 7
Mean value and SD of landslide susceptibility indices predicted by LR, MLP and SVM based unified, probability and maximum susceptibility methods.

Coupled model	Unified method		Probability method		Maximum susceptibility method	
	Mean	SD	Mean	SD	Mean	SD
LR	0.361	0.233	0.411	0.255	0.417	0.259
MLP	0.286	0.227	0.419	0.27	0.42	0.275
SVM	0.286	0.258	0.401	0.267	0.397	0.275

$_{\text{method}}$) > $SD_{(\text{Unified method})}$. On the whole, the mean values of the landslide susceptibility indices predicted by the unified method are relatively small, and the corresponding SDs are relatively large, indicating that the landslide susceptibility indices are concentrated in the very low and low susceptibility levels and the dispersion degree is large. It can be seen from Fig. 11 and Table 7 that the distributions of the three types of landslide susceptibility indices predicted by the LR, MLP and SVM models considering landslide types are basically consistent with those by the C5.0 decision tree model.

The receiver operating characteristic curves of LSP considering landslide types based on the LR, MLP and SVM models are also compared. Taking the SVM model as an example, the maximum AUC accuracy of LSP is obtained by the unified method (82.5%), followed by the probability method (81.3%) and the maximum susceptibility method (81%). Hence, the three coupled methods all have good abilities to identify landslides in the SVM model. The results of LR and MLP models are in accordance with those of SVM model. Furthermore, the receiver operating characteristic curves of the C5.0 decision tree model are similar to those of the LR, MLP and SVM models. However, the AUC accuracy of C5.0 decision tree based on the unified method (90.8%), probability method (86%) and maximum susceptibility method (85.6%) are higher than those of LR, MLP and SVM models.

6.2. Comparisons between single LSP and LSP considering landslide types

This section aims to discuss the uncertainties of the results predicted by the single LSP and the LSP considering landslide types based on the C5.0 decision tree with the best performance.

6.2.1. Comparisons of frequency ratio accuracy

The frequency ratios of rock fall, colluvial landslides and the landslides considering landslide types are listed in Tables 4 and 6 As shown in the tables, the frequency ratios of various coupled conditions gradually decrease. Among them, the frequency ratio accuracy of colluvial landslide susceptibility is 95.84%. Meanwhile, the landslide susceptibility considering landslide types predicted by the unified method has higher frequency ratio accuracy of 94.44%, followed by the probability method and the maximum susceptibility method, with frequency ratio accuracies of 88.65% and 88.45%, respectively. Finally, the frequency ratio accuracy of rock fall susceptibility is 86.17%. It shows that the frequency ratio accuracies of LSP considering landslide types under various coupled conditions are high.

6.2.2. Comparison of landslide susceptibility indices

As shown in Fig. 13a–e, the mean value ranking of susceptibility indices of rock fall and colluvial landslide and the susceptibility indices considering landslide types is $\text{Mean}_{(\text{Probability method})}$ > Mean $_{(\text{Maximum susceptibility method})}$ > Mean $_{(\text{Rock fall})}$ > Mean $_{(\text{Unified method})}$ > $\text{Mean}_{(\text{Colluvial landslides})}$. The corresponding SD ranking is $SD_{(\text{Colluvial landslides})}$ = $SD_{(\text{Maximum susceptibility method})}$ > $SD_{(\text{Unified method})}$ > $SD_{(\text{Probability method})}$ > $SD_{(\text{Rock fall})}$. On the whole, the mean values of the susceptibility indices under various conditions are small and the SDs are large, indicating that the landslide susceptibility indices predicted by the C5.0 decision tree are concentrated in the very low and low levels with high dispersion degree. Among them, the mean values of susceptibility indices under the rock fall,

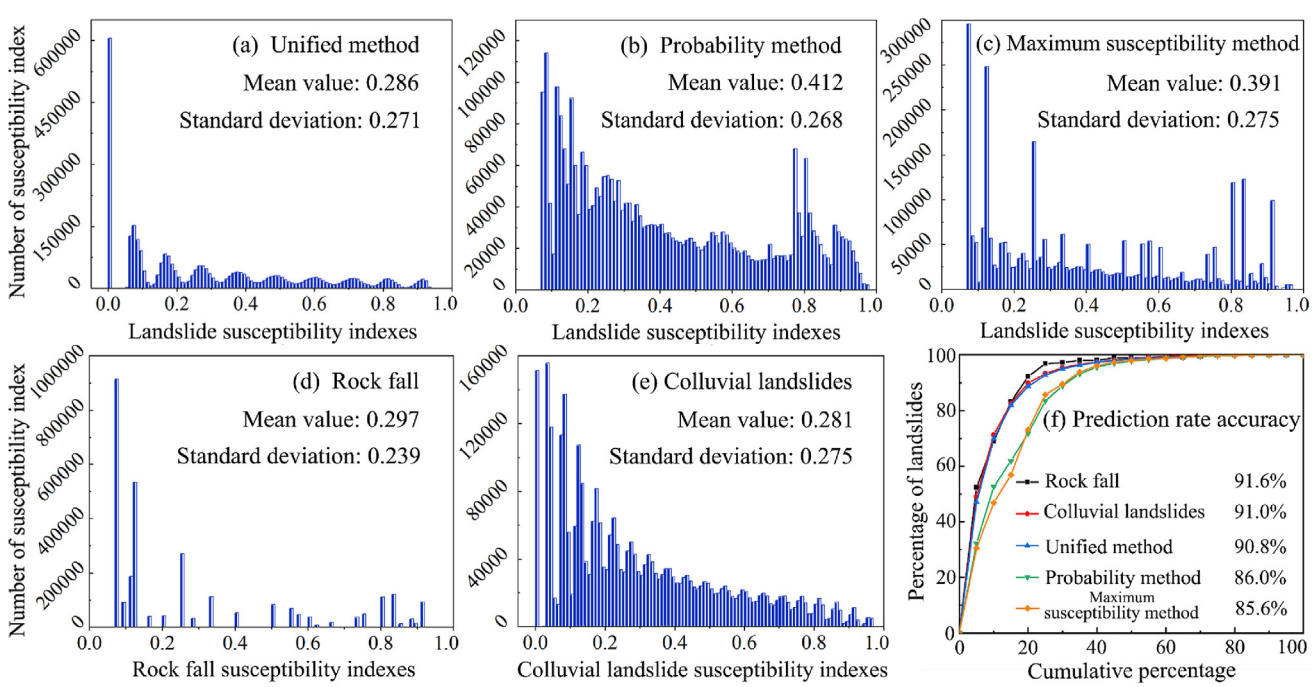

Fig. 13. Mean values and SD of landslide susceptibility indices predicted by the C5.0 decision tree based (a) unified method, (b) probability method, and (c) maximum susceptibility method; and the mean values and SD of (d) single rock fall and (e) colluvial landslide susceptibility indices predicted by the C5.0 decision tree, and (f) corresponding prediction rate accuracies.

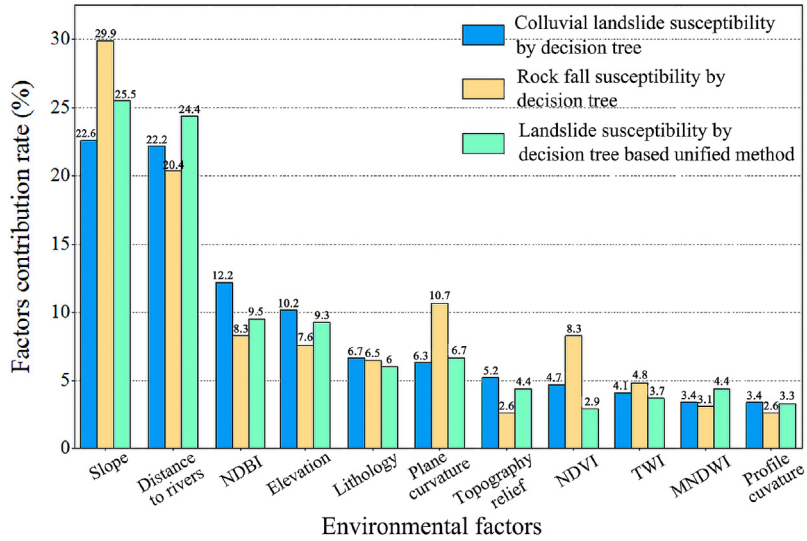

Fig. 14. Relative importance ranking of environmental factors under C5.0 decision tree model with different landslide types.

colluvial landslide and unified method are smaller than those under other conditions, and the corresponding SDs of colluvial landslide and unified method are larger. Furthermore, their susceptibility maps well indicate the differences between different grid units and use less high susceptibility indices to reflect abundant known landslide inventories.

6.2.3. Comparison of prediction rate accuracy

For the calculation of prediction rate accuracy, firstly, all types of susceptibility indices in the 3,001,146 grid units of the study area are firstly arranged in descending order. Then these susceptibility indices in descending order are divided into 20 parts at 5% intervals. Next, the number of landslide grid units that fall into different equal intervals is counted separately. Finally, the prediction rate curves are drawn by calculating the cumulative percentage of the landslide grid units in different equal intervals (Fig. 13f). As shown in Fig. 13f, the top 20% of various landslide grid units to account for the proportion of the C5.0 decision tree model are ranked as: Colluvial landslides (89.78%) > Unified method (88.74%) > Rock fall (87.01%) > Maximum susceptibility method (73.12%) > Probability method (71.82%). In very high and high susceptibility levels, the C5.0 decision tree model has a better ability to identify landslides. In addition, the prediction rate accuracy of rock fall is 91.6%, followed by the colluvial landslide (91%), unified method (90.8%), probability method (86%) and maximum susceptibility method (85.6%). Therefore, the prediction rate accuracies of LSP model considering landslide types are close to that of the rock fall and colluvial landslides susceptibility prediction.

6.3. Relative importance comparisons of environmental factors under different landslide types

The importance of environmental factors reflects the degree of their influence on landslide events in the study area (Reichenbach et al., 2018; Chang et al., 2022). Because of the highest LSP performance, the factor values calculated through the proposed C5.0 decision tree model are used to evaluate the importance of environmental factors (Liu et al., 2022). This paper plans to calculate the related importance of the 11 environmental factors under three different applications, including rock fall susceptibility prediction, colluvial landslide susceptibility prediction, and the unified method without considering landslide types. In addition, the probability method and maximum susceptibility method are not considered to be separately used, because both methods are coupled with the susceptibility predictions of rock fall and colluvial landslide.

It can be observed from Fig. 14 that the most important environmental factors for landslide events in all three applications include slope and distances to rivers. The contribution rate of slope factor is the highest during predicting rockfall susceptibility (29%), while those under colluvial landslide susceptibility and unified method are 22.6% and 25.5%, respectively. Under the condition of using the uniform method, the contribution rate of distance to rivers reaches a higher value of 24.4% than those under the conditions of predicting colluvial landslide (22.2%) and rock fall landslide (20.4%). Furthermore, the ranking of the next important environmental factors is also different from each other. For example, in terms of the next most important environmental factors affecting rockfall susceptibility, the ranking of contribution rates is plane curvature (10.7%), NDBI (8.3%) and NDVI (8.3%), those affecting the colluvial susceptibility are NDBI (12.2%), elevation (10.2%) and lithology (6.7%), and those affecting the united method are NDBI (9.5%), elevation (9.3%) and plane curvature (6.7%). It can be found from these comparisons that the ranking rules of the contribution rates of environmental factors under different landslide types have a certain degree of similarity in this study area, although there are differences in the contribution rate ranking among various types of landslides.

6.4. Discussion of LSP considering landslide types

Through comparisons of this case study, the distribution patterns of susceptibility indices predicted by the unified method, probability method and maximum susceptibility method based C5.0 decision tree models are generally similar. Among them, the unified method has the best LSP performance, followed by the probability method and the maximum susceptibility method. In addition, the prediction accuracies of landslide susceptibility considering landslide types in this study are not higher than those of single rock fall and/or colluvial landslide susceptibility. These conclusions are inconsistent with those of other scholars. For example, Guo et al. (2021) found that the prediction rate accuracy of the weighted frequency ratio model considering landslide types was better than that ignoring landslide types. Sun et al. (2020a) classified landslides in Xining City of China as soil landslides and

rock landslides to more accurately perform LSP, suggesting that the prediction rate accuracy considering landslide types has been significantly improved. Reasons for the differences between the conclusions in this study and related literature are as follows.

(1) Different study areas. The natural environmental conditions and engineering activities in various study areas are different. Therefore, the extracted environmental factors vary in the value scope, type and importance. Moreover, there are also differences in the number, type, instability mechanism and spatial extent of the non-landslide sample selection and triggering factors of landslides in various study area (Lin et al., 2021; Wang et al., 2022).
(2) Problem of data source acquisition. The spatial locations of rock fall and colluvial landslides may be inaccurately mapped and the environmental factors of rock fall and colluvial landslides may be inaccurately identified. The inaccuracies of these data sources will lead to inaccurate LSP. In addition, this study only extracts 11 types of environmental factors, which may be not enough to predict satisfied landslide susceptibility. Next, more abundant landslide environmental factors should be obtained from various data sources (Pawluszek and Borkowski, 2016; Lin et al., 2021).
(3) Few references related to the LSP study considering landslide types. It is found from relevant literature that most studies take a single type of landslide as examples to carry out LSP or do not consider the issue of different landslide types (Zhou et al., 2018; Mao et al., 2022). As a result, the LSP results considering landslide types lack sufficient comparative information. It is difficult to draw reliable conclusions only based on these limit study results.
(4) Assessment methods of LSP results still need to be considered. The uncertainties of the LSP results are only assessed from the perspectives of frequency ratio accuracy, susceptibility index distribution patterns and AUC accuracy. However, it may be necessary to assess the LSP results from more perspectives, such as Kendall test of synergy coefficient, field validation (Li et al., 2020a), and seed cell area indices (Süzen and Doyuran, 2004).
(5) Problem of coupled methods used for different landslide types. The unified method, probability method and maximum susceptibility method may have some problems. For example, the unified method does not take into account the differences of various landslide types and the universality of environmental factors in different types of landslides. The probability method may produce calculation errors when using probability formulae. Meanwhile, the maximum susceptibility method may amplify the errors of LSP results (Zhou et al., 2018).
(6) Unbalanced data quantity of different landslide types. The number of colluvial landslides (350) is greater than that of rock fall (105) in this study area. Therefore, during the unified process, the characteristics of rock fall may be influenced by the characteristics of colluvial landslides. Meanwhile, the final landslide susceptibility will be mainly characterized by those of colluvial landslides, while those of rock fall might be ignored. Even when the number of rock fall and colluvial landslides is equal, whether there will be changes in the results of the three coupled methods is open to question. In the next step, some methods can be chosen to handle unbalanced data, such as full convolutional network with focus loss (Süzen and Doyuran, 2004).
(7) There are some other landslide types. This study only couples two types of landslides, namely rock fall and colluvial landslides, to carry out LSP. However, there are more types of landslides, such as debris flows and rolling rocks in the study area (Hungr et al., 2014; Qiao et al., 2021). When we consider three or more types of landslides in LSP modeling, whether the errors inherent in the unified method or the maximum susceptibility method would reduce needs for further study.

These uncertain issues indicate that there are still improvement room in the LSP considering landslide types. Although this study shows that the unified method has the best performance for LSP considering landslide types, the probability method and maximum susceptibility method may be more consistent with the theoretical basis of LSP. It is recommended to perform further LSP verification in other study areas to compare the three coupled models. Therefore, future work will focus on replacing with other study areas, the improvement of the quality of data sources, extracting richer types of environmental factors, selecting different landslide types with a balanced number, coupling three or more different landslide types, and using more comprehensive methods to perform the LSP considering landslide types.

7. Concluding remarks

This study aims to construct LSP models that can consider different landslide types. The C5.0 decision tree model with efficient LSP performance is adopted to couple the unified method, probability method and maximum susceptibility method considering different landslide types. Finally, the uncertainties of various landslide susceptibility results are discussed.

It is concluded that the three LSPs considering landslide types conform to the occurrence patterns of landslides in the study area. Generally, the united method has the best performance in predicting susceptibility, followed by the probability method and maximum susceptibility method. Combined with the uncertainties of these LSPs considering landslide types, more case studies are needed to discuss the strengths and weaknesses of these coupled models. It can be seen from the comprehensive uncertainty comparison of colluvial landslide/rock fall susceptibility and landslide susceptibility considering landslide types that the performance of these susceptibility predictions also matches with each other on the whole. However, the landslide susceptibility considering different landslide types is obviously superior to those of single colluvial landslide or rock fall susceptibility, because it can more comprehensively reflect the evolution rules of landslides in the study area.

Declaration of competing interest

The authors declare that they have no known competing financial interests or personal relationships that could have appeared to influence the work reported in this paper.

Acknowledgements

This research is funded by the Natural Science Foundation of China (Grant Nos. 52079062 and 41807285), and the Interdisciplinary Innovation Fund of Natural Science, Nanchang University, China (Grant No. 9167-28220007-YB2107).

References

Aditian, A., Kubota, T., Shinohara, Y., 2018. Comparison of GIS-based landslide susceptibility models using frequency ratio, logistic regression, and artificial neural network in a tertiary region of Ambon, Indonesia. Geomorphology 318, 101–111.

Akgun, A., 2012. A comparison of landslide susceptibility maps produced by logistic regression, multi-criteria decision, and likelihood ratio methods: a case study at İzmir, Turkey. Landslides 9, 93–106.
Ayalew, L., Yamagishi, H., 2005. The application of GIS-based logistic regression for landslide susceptibility mapping in the Kakuda-Yahiko Mountains, Central Japan. Geomorphology 65, 15–31.
Bourenane, H., Bouhadad, Y., 2021. Impact of land use changes on landslides occurrence in urban area: the case of the Constantine City (NE Algeria). Geotech. Geol. Eng. 39, 1–21.
Brenning, A., 2005. Spatial prediction models for landslide hazards: review, comparison and evaluation. Nat. Hazards Earth Syst. Sci. 5, 853–862.
Bui, D.T., Tsangaratos, P., Nguyen, V.T., Liem, N.V., Trinh, P.T., 2020. Comparing the prediction performance of a deep learning neural network model with conventional machine learning models in landslide susceptibility assessment. Catena 188, 104426.
Cantarino, I., Carrion, M.A., Goerlich, F., Martinez Ibañez, V., 2018. A ROC analysis-based classification method for landslide susceptibility maps. Landslides 16, 265–282.
Cao, J., Zhang, Z., Wang, C., Liu, J., Zhang, L., 2019. Susceptibility assessment of landslides triggered by earthquakes in the western Sichuan Plateau. Catena 175, 63–76.
Chang, Z., Catani, F., Huang, F., Liu, G., Meena, S.R., Huang, J., Zhou, C., 2022. Landslide susceptibility prediction using slope unit-based machine learning models considering the heterogeneity of conditioning factors. J. Rock Mech. Geotech. Eng. https://doi.org/10.1016/j.jrmge.2022.07.009.
Chang, Z., Du, Z., Zhang, F., Huang, F., Chen, J., Li, W., Guo, Z., 2020. Landslide susceptibility prediction based on remote sensing images and GIS: comparisons of supervised and unsupervised machine learning models. Rem. Sens. 12 (3), 502.
Chen, W., Peng, J., Hong, H., Shahabi, H., Pradhan, B., Liu, J., Zhu, A.X., Pei, X., Duan, Z., 2018. Landslide susceptibility modelling using GIS-based machine learning techniques for Chongren County, Jiangxi Province, China. Sci. Total Environ. 626, 1121–1135.
Chen, X., Chen, W., 2021. GIS-based landslide susceptibility assessment using optimized hybrid machine learning methods. Catena 196, 104833.
Chung, C.J., Fabbri, A.G., 2008. Predicting landslides for risk analysis — spatial models tested by a cross-validation technique. Geomorphology 94, 438–452.
Dai, C., Li, W.L., Wang, D., Lu, H.Y., Xu, Q., Jian, J., 2021. Active landslide detection based on sentinel-1 data and InSAR technology in Zhouqu county, Gansu Province, Northwest China. J. Earth Sci. 32, 1092–1103.
Demir, G., 2019. GIS-Based landslide susceptibility mapping for a part of the North Anatolian fault zone between Reşadiye and Koyulhisar (Turkey). Catena 183, 104211.
Di Napoli, M., Di Martire, D., Bausilio, G., Calcaterra, D., Confuorto, P., Firpo, M., Pepe, G., Cevasco, A., 2021. Rainfall-induced shallow landslide detachment, transit and runout susceptibility mapping by integrating machine learning techniques and gis-based approaches. Water 13 (4), 488.
Farzam, A., Nollet, M.J., Khaled, A., 2018. Susceptibility modelling of seismically induced effects (landslides and rock falls) integrated to rapid scoring procedures for bridges using GIS tools for the Lowlands of the Saint-Lawrence Valley. Geomatics, Nat. Hazards Risk 9, 589–607.
Golkarian, A., Naghibi, S.A., Kalantar, B., Pradhan, B., 2018. Groundwater potential mapping using C5.0, random forest, and multivariate adaptive regression spline models in GIS. Environ. Monit. Assess. 190, 149.
Guo, Shi, Y., Huang, F., Fan, X., Huang, J., 2021. Landslide susceptibility zonation method based on C5.0 decision tree and K-means cluster algorithms to improve the efficiency of risk management. Geosci. Front. 12, 101249.
Guo, Z.Z., Yin, K.L., Huang, F.M., Fu, S., Zhang, W., 2019. Evaluation of landslide susceptibility based on landslide classification and weighted frequency ratio model. Chin. J. Rock Mech. Eng. 38 (2), 287–300 (in Chinese).
Guzzetti, F., Carrara, A., Cardinali, M., Reichenbach, P., 1999. Landslide hazard evaluation: a review of current techniques and their application in a multi-scale study, Central Italy. Geomorphology 31, 181–216.
He, S., Pan, P., Dai, L., Wang, H., Liu, J., 2012. Application of kernel-based Fisher discriminant analysis to map landslide susceptibility in the Qinggan River delta, Three Gorges, China. Geomorphology 171–172, 30–41.
He, X.L., Xu, C., Qi, W.W., Huang, Y.D., Cheng, J., Xu, X.W., Yao, Q., Lu, Y.K., Dai, B.Y., 2021. Landslides triggered by the 2020 Qiaojia M_w5.1 earthquake, Yunnan, China: distribution, influence factors and tectonic significance. J. Earth Sci. 32, 1056–1068.
Hong, H., Tsangaratos, P., Ilia, I., Loupasakis, C., Wang, Y., 2020. Introducing a novel multi-layer perceptron network based on stochastic gradient descent optimized by a meta-heuristic algorithm for landslide susceptibility mapping. Sci. Total Environ. 742, 140549.
Huang, F., Cao, Z., Guo, J., Jiang, S.H., Li, S., Guo, Z., 2020a. Comparisons of heuristic, general statistical and machine learning models for landslide susceptibility prediction and mapping. Catena 191, 104580.
Huang, F., Cao, Z., Jiang, S.H., Zhou, C., Huang, J., Guo, Z., 2020b. Landslide susceptibility prediction based on a semi-supervised multiple-layer perceptron model. Landslides 17, 2919–2930.
Huang, F., Chen, J., Liu, W., Huang, J., Hong, H., Chen, W., 2022b. Regional rainfall-induced landslide hazard warning based on landslide susceptibility mapping and a critical rainfall threshold. Geomorphology 408, 108236.
Huang, F., Tao, S., Li, D., Lian, Z., Catani, F., Huang, J., Li, K., Zhang, C., 2022a. Landslide susceptibility prediction considering neighborhood characteristics of landslide spatial datasets and hydrological slope units using remote sensing and GIS technologies. Rem. Sens. 14, 4436.
Huang, Y., Zhao, L., 2018. Review on landslide susceptibility mapping using support vector machines. Catena 165, 520–529.
Hungr, O., Leroueil, S., Picarelli, L., 2014. The Varnes classification of landslide types, an update. Landslides 11, 167–194.
Jiang, W., Rao, P., Cao, R., Tang, Z., Chen, K., 2017. Comparative evaluation of geological disaster susceptibility using multi-regression methods and spatial accuracy validation. J. Geogr. Sci. 27, 439–462.
Kalantar, B., Pradhan, B., Naghibi, S.A., Motevalli, A., Mansor, S., 2017. Assessment of the effects of training data selection on the landslide susceptibility mapping: a comparison between support vector machine (SVM), logistic regression (LR) and artificial neural networks (ANN). Geomatics, Nat. Hazards Risk 9, 49–69.
Kalantar, B., Ueda, N., Lay, U.S., Al-Najjar, H.A.H., Halin, A.A., 2019. Conditioning factors determination for landslide susceptibility mapping using support vector machine learning. In: Proceedings of IGARSS 2019 – 2019 IEEE International Geoscience and Remote Sensing Symposium. The Institute of Electrical and Electronics Engineer (IEEE), Piscataway, USA, pp. 9626–9629.
Kong, C., Tian, Y., Ma, X., Weng, Z., Zhang, Z., Xu, K., 2021. Landslide susceptibility assessment based on different machine learning methods in Zhaoping County of eastern Guangxi. Rem. Sens. 13 (18), 3573.
Korte, D.M., Shakoor, A., 2019. Landslide susceptibility and soil loss estimates for Drift Creek watershed, Lincoln County, Oregon. Environ. Eng. Geosci. 26 (2), 167–184.
Li, Q.N., Huang, D., Pei, S.F., Qiao, J.P., Wang, M., 2021. Using physical model experiments for hazards assessment of rainfall-induced debris landslides. J. Earth Sci. 32, 1113–1128.
Li, W., Fan, X., Huang, F., Chen, W., Hong, H., Huang, J., Guo, Z., 2020a. Uncertainties analysis of collapse susceptibility prediction based on remote sensing and GIS: influences of different data-based models and connections between collapses and environmental factors. Rem. Sens. 12, 4134.
Li, Y., Sheng, Y., Chai, B., Zhang, W., Zhang, T., Wang, J., 2020b. Collapse susceptibility assessment using a support vector machine compared with back-propagation and radial basis function neural networks. Geomatics, Nat. Hazards Risk 11, 510–534.
Lin, Q., Lima, P., Steger, S., Glade, T., Jiang, T., Zhang, J., Liu, T., Wang, Y., 2021. National-scale data-driven rainfall induced landslide susceptibility mapping for China by accounting for incomplete landslide data. Geosci. Front. 12, 268–282.
Liu, L.L., Zhang, J., Li, J.Z., Huang, F., Wang, L.C., 2022. A bibliometric analysis of the landslide susceptibility research (1999–2021). Geocarto Int. 37, 14309–14334.
Liu, Z., Gilbert, G., Cepeda, J.M., Lysdahl, A.O.K., Piciullo, L., Hefre, H., Lacasse, S., 2021. Modelling of shallow landslides with machine learning algorithms. Geosci. Front. 12, 385–393.
Lombardo, L., Tanyas, H., Huser, R., Guzzetti, F., Castro-Camilo, D., 2021. Landslide size matters: a new data-driven, spatial prototype. Eng. Geol. 293, 106288.
Mao, Y.M., Mwakapesa, D.S., Li, Y.C., Xu, K.B., Nanehkaran, Y.A., Zhang, M.S., 2022. Assessment of landslide susceptibility using DBSCAN-ADH and LD-EV methods. J. Mt. Sci. 19, 184–197.
Merghadi, A., Yunus, A.P., Dou, J., Whiteley, J., Thaipham, B., Bui, T., Avtar, R., Boumezbeur, A., Pham, B., 2020. Machine learning methods for landslide susceptibility studies: a comparative overview of algorithm performance. Earth Sci. Rev. 207, 103225.
Nsengiyumva, J.B., Luo, G., Amanambu, A.C., Mind'je, R., Habiyaremye, G., Karamage, F., Ochege, F.U., Mupenzi, C., 2019. Comparing probabilistic and statistical methods in landslide susceptibility modeling in Rwanda/Centre-Eastern Africa. Sci. Total Environ. 659, 1457–1472.
Pawluszek, K., Borkowski, A., 2016. Impact of DEM-derived factors and analytical hierarchy process on landslide susceptibility mapping in the region of Rożnów Lake, Poland. Nat. Hazards 86, 919–952.
Pradhan, B., Lee, S., Buchroithner, M.F., 2010. A GIS-based back-propagation neural network model and its cross-application and validation for landslide susceptibility analyses. Comput. Environ. Urban Syst. 34, 216–235.
Qiao, S.S., Qin, S.W., Sun, J.B., Che, W.C., Yao, J.Y., Su, G., Chen, Y., Nnanwuba, U.E., 2021. Development of a region-partitioning method for debris flow susceptibility mapping. J. Mt. Sci. 18, 1177–1191.
Reichenbach, P., Rossi, M., Malamud, B.D., Mihir, M., Guzzetti, F., 2018. A review of statistically-based landslide susceptibility models. Earth Sci. Rev. 180, 60–91.
Roberts, S., Jones, J.N., Boulton, S.J., 2021. Characteristics of landslide path dependency revealed through multiple resolution landslide inventories in the Nepal Himalaya. Geomorphology 390, 107868.
Sun, C., Ma, R., Shang, H., 2020c. Landslide susceptibility assessment in Xining based on landslide classification. Hydrogeol. Eng. Geol. 47 (3), 173–181 (in Chinese).
Sun, D., Xu, J., Wen, H., Wang, D., 2020a. Assessment of landslide susceptibility mapping based on Bayesian hyperparameter optimization: a comparison between logistic regression and random forest. Eng. Geol. 281, 105972.
Sun, D., Xu, J., Wen, H., Wang, Y., 2020b. An optimized random forest model and its generalization ability in landslide susceptibility mapping: application in two areas of Three Gorges Reservoir, China. J. Earth Sci. 31, 1068–1086.

Süzen, M.L., Doyuran, V., 2004. A comparison of the GIS based landslide susceptibility assessment methods: multivariate versus bivariate. Environ. Geol. 45, 665–679.
Wang, C., Lin, Q., Wang, L., Jiang, T., Su, B., Wang, Y., Mondal, S.K., Huang, J., Wang, Y., 2022. The influences of the spatial extent selection for non-landslide samples on statistical-based landslide susceptibility modelling: a case study of Anhui Province in China. Nat. Hazards 112, 1967–1988.
Wang, X., Zhang, C., Wang, C., Liu, G., Wang, H., 2021. GIS-based for prediction and prevention of environmental geological disaster susceptibility: from a perspective of sustainable development. Ecotoxicol. Environ. Saf. 226, 112881.
Wang, Z., Liu, Q., Liu, Y., 2020. Mapping landslide susceptibility using machine learning algorithms and GIS: a case study in Shexian County, Anhui Province, China. Symmetry 12 (12), 1954.
Wca, B., Shuai, Z., 2021. GIS-based comparative study of Bayes network, Hoeffding tree and logistic model tree for landslide susceptibility modeling. Catena 203, 105344.
Zhang, Y., Tang, J., Cheng, Y., Huang, L., Guo, F., Yin, X., Li, N., 2022. Prediction of landslide displacement with dynamic features using intelligent approaches. Int. J. Min. Sci. Technol. 32 (3), 539–549.
Zhao, H., Tian, Y., Guo, Q., Li, M., Wu, J., 2020. The slope creep law for a soft rock in an open-pit mine in the Gobi region of Xinjiang, China. Int. J. Coal Sci. Technol. 7, 371–379.
Zhou, C., Yin, K., Cao, Y., Ahmed, B., Li, Y., Catani, F., Pourghasemi, H.R., 2018. Landslide susceptibility modeling applying machine learning methods: a case study from Longju in the Three Gorges Reservoir area, China. Comput. Geosci. 112, 23–37.

Faming Huang obtained his BSc degree in Geographic Information System from Taiyuan University of Technology, Taiyuan, China in 2011, and his MSc and PhD degrees in Geological Engineering from China University of Geosciences, Wuhan, China in 2013 and 2017, respectively. His research interests include: (1) failure mechanism analysis of engineering and natural hazards; (2) landslide stability and reliability analysis; (3) landslide susceptibility, hazard and risk mapping; (4) machine learning and numerical simulation in geological engineering; and (5) remote sensing and geographic information system.